



Universidade de Aveiro
2017

Departamento de Eletrónica,
Telecomunicações e Informática

**Pedro Miguel
Serrão Lopes**

**Técnicas de Transmissão e Recepção para Sistemas
MIMO Heterogéneos na banda das Ondas Milimétricas**

**Hybrid Transmit and Receive Designs for Massive MIMO
Millimeter-Wave Heterogeneous Systems**

Dissertação apresentada à Universidade de Aveiro para cumprimento dos requisitos necessários à obtenção do grau de Mestre em Engenharia Eletrónica e Telecomunicações, realizada sob a orientação científica do Doutor Adão Paulo Soares da Silva, Professor Auxiliar do Departamento de Eletrónica, Telecomunicações e Informática da Universidade de Aveiro e do Doutor Daniel Filipe Marques Castanheira, Investigador no Instituto de Telecomunicações de Aveiro

Part of this work was supported through the project SWING2 (PTDC /EEITEL/3684/2014), funded by Fundos Europeus Estruturais e de Investimento (FEEI) through Programa Operacional Competitividade e Internacionalização - COMPETE 2020 and by the National Funds from FCT - Fundação para a Ciência e a Tecnologia, through project POCI-01-0145-FEDER-016753.

o júri

presidente

Prof. Doutor Telmo Reis Cunha,
Professor Auxiliar na Universidade de Aveiro

arguente externo

Prof. Doutor Marco Alexandre Cravo Gomes,
Professor Auxiliar na Faculdade de Ciências e Tecnologia da Universidade de Coimbra

vogal

Prof. Doutor Adão Paulo Soares da Silva
Professor Auxiliar na Universidade de Aveiro

agradecimentos

Ao meu orientador Prof. Doutor Adão Silva e coorientador Doutor Daniel Castanheira, cujo conhecimento, apoio e criticismo foram indispensáveis para a realização deste trabalho.

Aos meus pais, já que sem o seu apoio não seria possível fazer este percurso académico com tamanho conforto.

Aos meus amigos, Prof. Carolina, Dra. Laura, Eng.º Marco, Alf. Miguel e Dra. Sara pelo tempo despendido para a revisão desta dissertação.

Aos professores da Universidade de Aveiro, pela motivação, profissionalismo e conhecimento transmitido.

Por último, um obrigado à restante família e amigos que tornaram esta jornada mais agradável.

palavras-chave

5G, LTE-Advanced, Massive MIMO, Ondas Milimétricas, Redes Heterogêneas, Comunicações Móveis, Arquiteturas Híbridas, Beamforming, Cognitive Radio, Alinhamento de Interferências.

resumo

Com o crescimento dos dispositivos de comunicações móveis e de serviços de banda larga, os requisitos do sistema tornam-se cada vez mais exigentes. O LTE-Advanced apresenta um melhoramento progressivo relativamente ao seu antecessor LTE, introduzindo redes heterogêneas, que têm vindo a provado ser uma solução sólida para melhorar tanto a capacidade, como a cobertura da rede.

Quanto à implementação do 5G, será necessário um salto disruptivo na tecnologia, o que permita novas possibilidades, tal como a de conectar pessoas e coisas. Para tornar isso possível, é necessário investigar e testar novas tecnologias. MIMO massivo e comunicações em ondas milimétricas são algumas das tecnologias que têm vindo a demonstrar resultados com potencial, tais como o aumento da capacidade e da eficiência espectral.

No entanto, devido às limitações na propagação de ondas milimétricas, a existência de cenários com redes heterogêneas ultradensas é uma possibilidade. Ao se considerar cenários ultradensos com um número massivo de utilizadores, o sistema fica limitado devido à interferência, mesmo operando na banda das ondas milimétricas. Como tal, é de extrema importância o desenvolvimento de técnicas que mitiguem essa interferência.

Nesta dissertação, propõe-se uma arquitetura de baixa complexidade para um transmissor e um recetor a operarem no sentido ascendente, numa rede heterogênea ultradensa. Nesta arquitetura são aplicadas tecnologias como MIMO massivo, ondas milimétricas e técnicas de beamforming, com o intuito de mitigar a interferência entre células. Usando a probabilidade de erro de bit como métrica de performance, os resultados mostram que a arquitetura proposta consegue remover a interferência eficientemente, alcançando resultados próximos de uma arquitetura completamente digital.

keywords

LTE-Advanced, 5G, Massive MIMO, Millimeter Wave Communications, Heterogeneous Networks, Mobile Communications, Hybrid Architectures, Beamforming, Cognitive Radio, Interference Alignment.

abstract

With the constant increase of mobile communication devices and broadband services, the system requirements are getting more demanding. Long Term Evolution (LTE) Advanced comes as a progressive enhancement to its predecessor LTE, introducing heterogeneous networks (HetNets), which have proven to be great solutions to improve both capacity and coverage. As for 5G, it takes more of a disruptive step, enabling new possibilities, such as connecting people and things. To enable such a step, new technologies and techniques need to be researched and tested. Massive Multiple-Input Multiple-Output (MIMO) and millimeter wave (mmWave) communications are two of such technologies, as they show promising results such as increased capacity and spectral efficiency. However, due to the mmWave propagation constraints, the existence of ultra-dense HetNet scenarios may be a possibility. When considering ultra-dense scenarios with a massive number of users, the system becomes interference-limited, even using mmWave band. As such, the design of interference mitigation techniques that deal with both inter and intra-tier interference are of the utmost importance.

In this dissertation, a low complexity analog-digital hybrid architecture for both the transmitter and receiver in the uplink scenario is proposed. It is designed for an ultra-dense heterogeneous system and employing massive MIMO, mmWave and beamforming techniques in order to mitigate both intra- and inter-tier interference. Considering the Bit Error Rate (BER) as the performance metric, the results show that the proposed architecture efficiently removes both inter- and intra-tier interferences, achieving a result close to its fully digital counterpart.

Index

1. Introduction.....	1
1.1. From the 1G to the 4G of Mobile Communications.....	1
1.2. Future 5G Mobile Communications	4
1.3. Motivation and Objectives.....	6
1.4. Contributions	8
1.5. Outline	9
1.6. Notation	10
2. LTE-Advanced and Heterogeneous Networks	11
2.1. LTE Advanced.....	11
2.1.1. Network Architecture	12
2.1.2. LTE multiple access techniques.....	13
2.1.3. Carrier Aggregation.....	18
2.1.4. MIMO Techniques	19
2.1.5. Coordinated Multipoint (CoMP).....	20
2.2. Heterogeneous Networks.....	22
2.2.1. Possible Deployment Scenarios	22
3. MIMO Systems.....	25
3.1. Multi-antenna types	25
3.1.1. SISO System	25
3.1.2. SIMO System	26
3.1.3. MISO System	26
3.1.4. MIMO System.....	27
3.2. Diversity	27

3.2.1.	Receive Diversity	28
3.2.2.	Transmit Diversity.....	29
3.3.	Spatial Multiplexing	31
3.3.1.	Channel Known at the Transmitter	32
3.3.2.	Channel Not Known at the Transmitter	33
4.	Massive MIMO with mmWave Communications.....	35
4.1.	Massive MIMO systems.....	35
4.1.1.	Benefits and Limitations of Massive MIMO	36
4.2.	Millimeter Wave Communications	37
4.2.1.	Benefits and Limitations of Millimeter Wave Communications	37
4.2.2.	Benefits of mmWave massive MIMO Systems	39
4.2.3.	Benefits of mmWave massive MIMO Systems in HetNets.....	40
4.3.	MmWave Massive MIMO Beamforming Architectures.....	41
4.3.1.	Digital Beamforming.....	41
4.3.2.	Analog Beamforming	42
4.3.3.	Hybrid Beamforming	42
5.	Hybrid Beamforming Designs for Massive MIMO mmWave Heterogeneous Systems	47
5.1.	System Model.....	48
5.1.1.	User Terminal Architecture.....	50
5.1.2.	Receiver Architecture.....	50
5.1.3.	Channel Model	52
5.2.	Hybrid Precoder and Equalizer Design	53
5.2.1.	Analog Equalizer and Precoder Design	53
5.2.2.	Digital Equalizer Design	58
5.2.3.	Digital Precoder Design	59

5.3. Simulation and Results	61
6. Conclusion and Future Work.....	67
6.1. Conclusion.....	67
6.2. Future Work.....	68
References.....	69

List of Figures

Figure 1.1. Mobile Communications Evolution [1].	2
Figure 1.2. Global mobile subscriptions by technology 2010-2017 [4].	5
Figure 1.3: 5G requirements and areas to address [6].	6
Figure 2.1. LTE-Advanced E-UTRAN and EPC architecture [31].	12
Figure 2.2. OFDM multiple sub-carriers and OFDM symbol [33].	14
Figure 2.3. CP operation [34].	14
Figure 2.4. FDD LTE frame structure [34].	15
Figure 2.5. TDD LTE frame structure [35].	16
Figure 2.6. Resource Block with 1.4 MHz bandwidth and normal CP (short) [36].	17
Figure 2.7. SC-FDMA and OFDMA data transmission [38].	18
Figure 2.8. Carrier Aggregation in FDD [39].	19
Figure 2.9. CoMP Centralized/Decentralized Control [41].	20
Figure 2.10. Downlink CoMP transmission [42].	21
Figure 2.11. Traditional network deployment with frequency re-use [45].	23
Figure 2.12. Example of a Heterogeneous Network.	24
Figure 3.1. SISO system.	26
Figure 3.2. SIMO system.	26
Figure 3.3. MISO system.	27
Figure 3.4. MIMO system.	27
Figure 3.5. SIMO Receive Diversity	28
Figure 3.6. MISO transmit diversity.	29
Figure 3.7. Block Diagram of the Alamouti space-time decoder [51].	31
Figure 3.8. MIMO system.	32
Figure 4.1. Example of massive MIMO operation [56].	36
Figure 4.2. Atmospheric absorption [62].	39
Figure 4.3. Variation of the coherence with the beamwidth [64].	40
Figure 4.4. Possible mmWave massive MIMO HetNet system [65].	40
Figure 4.5. MmWave massive MIMO system using digital beamforming [66]	41

Figure 4.6. MmWave massive MIMO system using analog beamforming [66].	42
Figure 4.7. MmWave massive MIMO system based on hybrid analog-digital precoding and combining [66].	43
Figure 4.8. Analog processing for hybrid beamforming based on phase shifters [66]: (a) each RF chain is connected to all the antennas; (b) each RF chain is connected to a subset of antennas.	43
Figure 4.9. Analog processing for hybrid beamforming based on switches [66]: (a) Each RF chain can be connected to all antennas; (b) each RF chain can be connected to a subset of antennas.	44
Figure 4.10. The CAP-MIMO transceiver that uses a lens-based front end for analog beamforming; it maps the $p=N_s$ precoded data streams to $L = O(+)$ beams via the mmWave beam selector and lens [66].	45
Figure 5.1. System model, example with 2 small cells within the macro-cell	49
Figure 5.2. User terminal block diagram	50
Figure 5.3. Block diagram of macro-cell receiver	51
Figure 5.4. Central unit block diagram	51
Figure 5.5. Macro-cell average BER for the first scenario	64
Figure 5.6. Small cell average BER for the first scenario.	64
Figure 5.7. Macro-cell average BER for the second scenario.	65
Figure 5.8. Small-cell average BER for the second scenario.	66

List of Tables

TABLE 1.I..... 3
TABLE 1.II..... 3
TABLE 2.I..... 16
TABLE 2.II..... 23
TABLE 3.I..... 30
TABLE 5.I: Parameters for the two different scenarios..... 61
TABLE 5.II: Precoder/equalizer designs..... 62

Acronyms

1G	1 st Generation
2G	2 nd Generation
3G	3 rd Generation
3GPP	3 rd Generation Partnership Project
4G	4 th Generation
5G	5 th Generation
AMPS	Advanced Mobile Phone Service
AP	Access Point
BER	Bit-Error-Rate
BS	Base Station
CAP	Continuous Aperture Phased
CDMA	Code-Division Multiple Access
CoMP	Coordinated Multi-Point
CP	Cyclic Prefix
CSI	Channel State Information
CU	Central Unit
D2D	Device to Device
DoF	Degree of Freedom
DwPTS	Downlink Pilot Time Slot
EDGE	Enhanced Data Rates for GSM Evolution
EGC	Equal Gain Combining

EPC	Evolved Packet Core
E-UTRAN	Evolved Universal Terrestrial Radio Access Network
FDD	Frequency Division Duplexing
FDMA	Frequency-Division Multiple Access
GP	Guard Period
GPRS	General Packet Radio Service
GSM	Global System for Mobile Communications
HetNets	Heterogeneous Networks
HSPA	High Speed Packet Access
ICI	Intercell Interference
IoT	Internet of Things
IP	Internet Protocol
ISI	Intersymbol Interference
ITU-R	International Telecommunications Union for Radio
LTE	Long Term Evolution
M2M	Machine to Machine
MAC	Media Access Control
MIMO	Multiple-Input Multiple-Output
MISO	Multiple-Input Single-Output
MME	Mobility Management Entity
MMSE	Minimum Mean Square Error
mmWave	Millimeter Wave
MRC	Maximal Ratio Combining
MU-MIMO	Multiple-User Multiple-Input Multiple-Output
NTT	Nippon Telegraph and Telephone

NMT	Nordic Mobile Telephone
OFDM	Orthogonal Frequency-Division Multiplexin
OFDMA	Orthogonal Frequency-Division Multiple Access
PA	Power Amplifier
PAPR	Peak-to-Average Power Ratio
P-GW	Packet Data Network Gateway
QAM	Quadrature Amplitude Modulation
RAN	Radio Access Network
RF	Radio-Frequency
RRE	Remote Radio Equipment
SC	Selection Combining
SC-FDMA	Single-Carry Frequency Division Multiple Access
SFBC	Space Frequency Block Coding
S-GW	Serving-Gateway
SIMO	Single-Input Multiple-Output
SISO	Single-Input Single-Output
SMS	Short Message Service
SNR	Signal-to-Noise Ratio
STBC	Space Time Block Coding
SU-MIMO	Single-User Multiple-Input Multiple-Output
SVD	Singular Value Decomposition
TACS	Total Access Communications System
TDD	Time Division Duplexing
TDMA	Time-Division Multiple Access
UE	User Equipment

UMTS	Universal Mobile Telecommunications System
UpPTS	Uplink Pilot Time Slot
UT	User Terminal
ZF	Zero Forcing



Chapter 1

Introduction

As humans rely on each other to thrive, the need for communication has been a key aspect throughout history. Conveying complex and secure information at short range has been easy since language was developed. However, for long distance communications, resourceful methods had to be put to practice. When humanity was fragmented throughout the globe, distance communication was only needed for small and restricted geographical areas. As such, people would rely on loud sound sources (horns, drums) or visible signals (fire, smoke), which could only convey a very limited amount of information. With the development of writing and as civilizations emerged, expanded and connected, the need to convey more complex information arose. Systems that could deliver written messages were developed, but always limited by the velocity of the carrier. As we approach modern times, communication systems working at the speed of light are developed, such as the telegraph or the telephone, although constrained by the need of wires. It is only in 1896 when Guglielmo Marconi patents the first wireless communication system. Since then, wireless communications systems have evolved from point-to-point communications to a whole wireless network connecting the globe.

1.1. From the 1G to the 4G of Mobile Communications

As mobile communications at their earliest were done solely in the analog domain, it took some years until it became commercially viable. These early systems required high power and large bandwidths, severely limiting its capacity. With the development of



techniques such as the cellular concept and the frequency reuse by Bell Labs, it was possible to achieve a greater coverage area and capacity. A brief illustration of the mobile communications evolution can be seen on Figure 1.1.

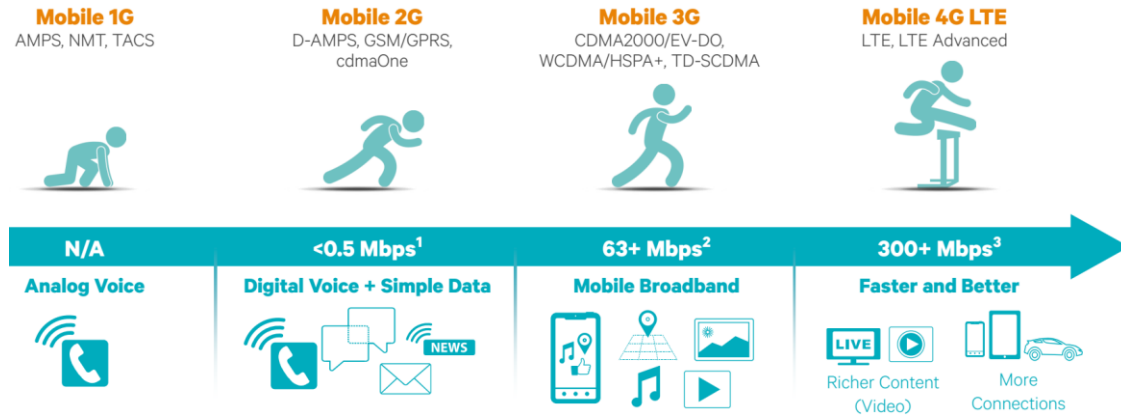


Figure 1.1. Mobile Communications Evolution [1].

1G

The 1G systems were completely analogic and used frequency-division multiple access (FDMA). Even though these systems were a big leap for the time, they were extremely inefficient. They were bulky, both spectrum and power inefficient, expensive, only allowed one user per channel and were susceptible to interference. To add to that, as the systems were developed and deployed independently, each had their own standards, making them incompatible with each other. Some of the firstly deployed systems can be seen in TABLE 1.I.

2G

In the early 90s, 2G systems brought major improvements relatively to its predecessor 1G as it transitioned from analog to digital. With this, a longer battery life, smaller and cheaper mobile phones were made possible, which contributed to a rapid increase of mobile users. The communications also got more robust to interference and data transmission became possible (e.g. Short Message Service (SMS)). The introduction of multiple access technologies based on time-division multiple access (TDMA) and code-division multiple access (CDMA) greatly increased the system's capacity and spectrum efficiency, as it allowed to serve multiple users per channel. TABLE 1.II shows



the main 2G mobile systems, most of them working over Frequency Division Duplexing (FDD), in which both the transmitter and receiver operate at different frequency bands.

TABLE 1.I
1G MOBILE SYSTEMS

Year	System	Country
1979	Nippon Telegraph and Telephone (NTT)	Japan
1981	Nordic Mobile Telephone (NMT)	Finland, Denmark, Sweden, Norway
1982	Advanced Mobile Phone Service (AMPS)	USA
1983	Total Access Communication System (TACS)	UK

TABLE 1.II
2G MOBILE SYSTEMS

System	Country	Multiple Access Technology
Personal Digital Cellular (PDC)	Japan	TDMA/FDD
GSM	Europe	TDMA/FDD
cdmaOne	USA	CDMA
Digital AMPS	N. America & South Korea	TDMA/FDD

2.5G

As the number of mobile users and data services kept increasing, 2G started to lag behind in face of the demands. To cope with this problem, in the early 00s, 2.5G was introduced to enhance the currently deployed 2G network. The two enhancements made to the Global System for Mobile Communications (GSM) network, the most globally used system, were the addition of the General Packet Radio Service (GPRS), which allowed the current system to support packet services, and later of the Enhanced Data Rates for GSM Evolution (EDGE), which increased the current system's data rates.



Due to their success, 2G and 2.5G networks achieved a great coverage area throughout the world and survived till today. However, network providers are now shutting down their 2G networks [2], [3], as the technology is outdated and the number of users keeps decreasing. But even so, it keeps surviving in some places, such as is in Europe, due to its recent use on Internet of Things (IoT) applications, although its days are numbered, as other more suitable IoT technologies also emerge in the market.

3G

With the proliferation of the internet throughout the world and with the potential exploitation of broadband data services, a new technology was needed to accommodate these demands. As a solution, 3G was developed by the 3G Partnership Project (3GPP) group and introduced in the mid-00s, with the standards Universal Mobile Telecommunications System (UMTS) and CDMA2000. The main differences from the previous technology (2G), were the increase in the data rate and the use of packet switching instead of circuit switching for data transmission. This technology kept getting enhanced throughout the years with technologies like High Speed Packet Access (HSPA) which allowed greater data rate speeds and capacity.

4G

As the end of the decade approached, 4G started to be introduced as the next decade's technology. Some requirements were set by the International Telecommunications Union for Radio (ITU-R), such as 100 Mbit/s data rates in high mobility environments and 1 Gbit/s in low mobility or a simplified all-IP architecture. However, the first candidates (HSPA+ and LTE), which brought major improvements to 3G, failed to meet those requirements, but were nonetheless commercialized as 4G. Afterwards, one of those candidates, LTE, which was developed by the 3GPP group, underwent a major enhancement, originating in LTE-Advanced, which met the requirements set for 4G. Since it was introduced in the market, the number of LTE subscribers keeps increasing, replacing the older technologies, as depicted in Figure 1.2.

1.2. Future 5G Mobile Communications

As seen in the previous chapter, a new generation of mobile communications technology is introduced approximately every 10 years. As we are approaching the 10 year mark from the previous generation (4G), discussion on what 5G should be emerges.

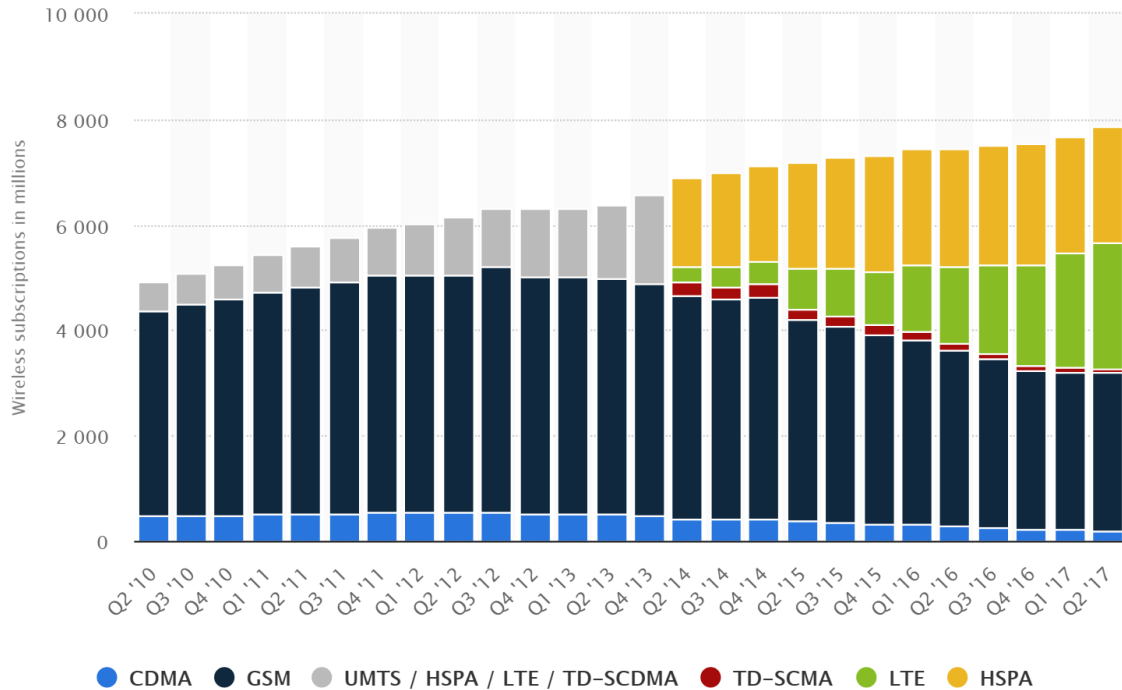


Figure 1.2. Global mobile subscriptions by technology 2010-2017 [4].

Efforts are being made on research for potential technologies and, as in 4G, the ITU-R set some requirements [5] for what 5G should achieve.

Whereas the previous generations focused on connecting people, 5G will go beyond that and will aim to connect both people and things. Keeping up with the currently growing high quality media services, smart factories, autonomous driving and immersive augmented reality are some of the possible usages unlocked by 5G. To enable this potential and cope with the industry's demands, three areas must be addressed, massive internet of things applications, mission-critical control and enhanced mobile broadband, each with its requirements, as seen in Figure 1.3.

However, to achieve all this, new technologies are needed. Those technologies will not try to solve all the aforementioned requirements, but some specific ones. Some of these technologies are as follows:

- Network densification, which will make use of cells of smaller sizes to cover specific areas, allowing for a better spectrum and energy efficiency and increased data rates and connection capacity [7], [8].
- Full-Duplex, in which by allowing the down and up link to work over a single channel, the spectrum efficiency would double [9].



- Device-to-Device (D2D) and Machine-to-Machine (M2M) communications, which will allow to off-load the network and evolve towards the internet of things (IoT) [10].
- MmWave, which, by taking advantage of the unused spectrum at higher frequencies, with the wavelength in the order of millimeters (from around 20GHz to 300GHz), makes possible to achieve high transmission rates and a reduced antenna size [11].
- Massive MIMO, where a massive number of antennas is deployed on a base station (BS) [12].
- Network Virtualization, where a distribution of datacenters aids the network [13].
- Cognitive radio, which by adding intelligence to the network makes it possible to use the spectrum more efficiently [14].

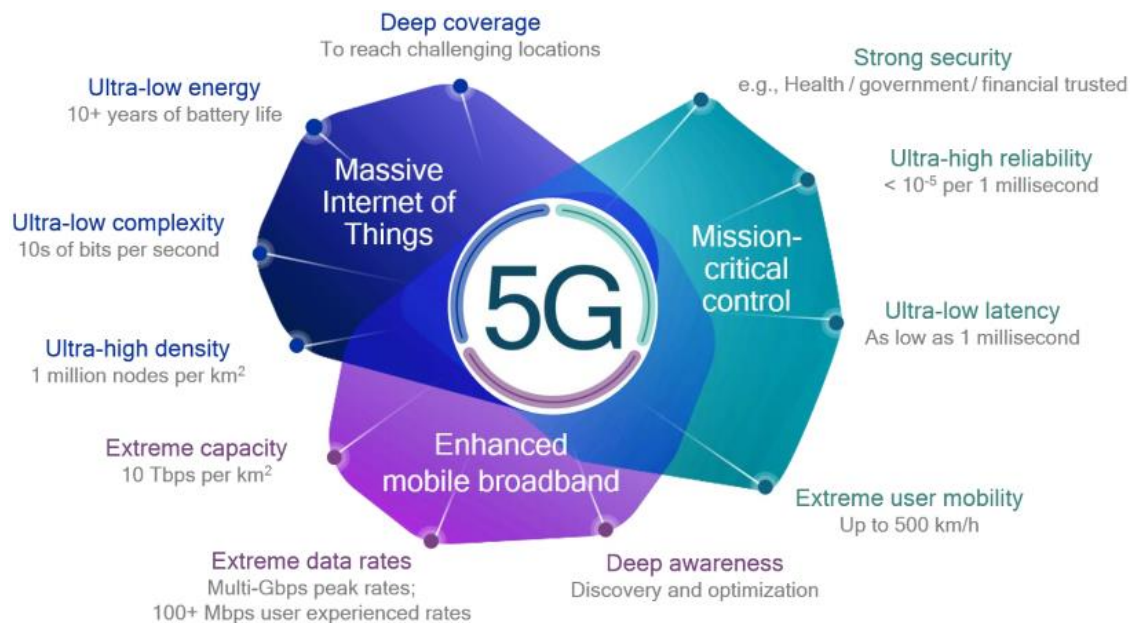


Figure 1.3: 5G requirements and areas to address [6].

1.3. Motivation and Objectives

4G mobile communication systems, also known as Long-Term-Evolution (LTE) [15], recently deployed in the Portuguese market, allow for much greater data rates than its predecessor 3G. However, the predictable increase in the need for broadband services, which require high data rates, cannot be met with the current network architecture. In a



cellular network, a way to increase the data rates would be to reduce the cell's size, consequently decreasing the propagation losses. The densification of the network, which implies the introduction of small-cells in the macro-cell, is already considered as a viable and flexible option to increase the capacity of the system by the network operators. However, due to the high cost of new spectrum acquisition licenses, it is expected that both the macro and small-cell operate at the same frequency. This results in a great increase in the interference between both systems. Since the macro-cell is the owner of the spectrum license, the small-cells must use the system resources in a way that they do not damage the system's performance for the users in the macro-cell.

Small-cells can also make use of techniques which are being researched, such as massive MIMO and mmWave [16]–[18]. Where massive MIMO makes use of a massive number of antennas to exploit the available spatial resources, while mmWave opens a whole new free spectrum at high frequencies, with the possibility of much higher data rates, in the order of multi-gigabit per second [17]. However, the wireless propagation characteristics are quite different from the current sub-6GHz band [19], [20], as it degrades with the increase in frequency. As such, special care is needed when designing beamforming schemes [21]. As a way to make the most out of the available resources, the introduction of cognitive capabilities in the small-cells is of the utmost importance. Since from the detection of system parameters, the small-cells can adapt to the current conditions. As such, it will be necessary to develop detection techniques, as well as methods which will allow to better manage the available resources in heterogeneous system (systems with both macro and small-cells).

Combining both technologies, mmWave and massive MIMO, brings some benefits, as it allows to pack a higher number of antennas into the same volume, if compared to lower frequencies, due to the small wavelength of the mmWaves [22]. Therefore, both terminals can be equipped with a massive number of antennas, which will allow designing efficient beamforming techniques that can compensate for the attenuation at higher frequencies. However, the design of these beamforming techniques should follow different approaches from the ones adopted for its lower frequency counterparts, mainly due to hardware limitations [23]. Due to their limitations, hybrid analog-digital beamforming techniques, where some processing is done at both the digital and analog level, are being researched [24]–[27].



As noted in [28], the use of mmWave and massive MIMO in the context of heterogeneous networks would be a key factor to increase the network capacity for future 5G networks. For a low dense scenario and due to the short range of mmWave communications, it is expected that the users on a given small cell would not interfere with other small cells and macro cells, and the system is mainly noise-limited. However, in ultra-dense scenarios with a massive number of users the system becomes interference-limited, even using the mmWave band [29] since at the mmWave band, the channel shows significant differences for line-of-sight (LOS) and non-line-of-sight (NLOS) path loss characteristics. For example, channel measurements show a path loss exponent of approximately 2 for LOS and an exponent as large as 5.76 in downtown New York City [11]. As shown in [29], when the density of the network is very high (for example, in ultra-dense networks) the interference is significant, since that for ultra-dense scenarios, a user sees several LOS base stations and thus experiences significant interference. As mentioned in [29], the development of more advanced interference management techniques is an interesting topic for ultra-dense massive MIMO mmWave-based networks.

This dissertation is inserted in the wireless mobile communications field, and has as an objective, to study, implement and evaluate the performance of an ultra-dense heterogeneous system where both primary users (macro-cell) and secondary users (small-cell) coexist under the same spectrum. The work consists on developing hybrid analog-digital precoding techniques, considering different knowledge of the channel state information (CSI). Specifically, the aim is to design a low complexity hybrid analog-digital transmit precoding and receive equalizer for uplink massive MIMO mmWave ultra-dense heterogeneous networks.

1.4. Contributions

In this dissertation, the design of a low complexity hybrid analog-digital transmit and receive beamforming (or precoder/equalizer) for ultra-dense uplink massive MIMO mmWave HetNets networks was successfully developed. To this date, and to the best knowledge of the author, uplink hybrid beamforming approaches designed for massive MIMO mmWave in the context of HetNets has not been addressed in the literature. Also, as a result of this work, the following article has been published [30]:



D. Castanheira, P. Lopes, A. Silva, A. Gameiro, “Hybrid Beamforming Designs for Massive MIMO Millimeter-Wave Heterogeneous Systems”, *IEEE Access*, vol. 5, no. 1, pp. 21806 - 21817, Nov 2017.

1.5. Outline

This dissertation started by providing a contextualization on the mobile communications technology and briefly introduced the work developed and the motivation behind it. This work is comprised of 5 more chapters.

Chapter 2 introduces LTE and LTE-Advanced by giving an overview of their technologies, with special focus on heterogeneous networks. After a brief introduction, the chapter starts by describing the system’s network architecture, going over the used multiple access techniques, carrier aggregation, and then, HetNets.

Chapter 3 explains the concept of using multiple antennas for communications, with special focus on the techniques used for LTE. The chapter starts by introducing the possible multi-antenna types. Then, the diversity and multiplexing concepts are introduced and techniques on how they can be applied to multi-antenna systems are presented.

Chapter 4 gives an overview of the current state of massive MIMO and mmWave communications. The chapter goes over the benefits and limitations of both technologies, and how they can be combined. At the end of the chapter, possible architectures to employ both techniques are presented.

Chapter 5 covers the work developed and the obtained results. It starts by introducing the system model, describing the scenario, both the receiver and transmitter architecture and the channel model. Then, besides the proposed design, various analog/digital precoders and equalizers are presented. Furthermore, it shows and compares the obtained results for different combinations of analog/digital precoders and equalizers, as well as different scenarios, with BER as the performance metric.

Chapter 6 summarizes the main ideas and conclusions of the developed work, as well as the contributions made and possible future work.



1.6. Notation

Boldface capital letters denote matrices and boldface lowercase letters denote column vectors. The operations $(.)^T$, $(.)^H$, $(.)^*$ and $tr(.)$ represent the transpose, the Hermitian transpose, the conjugate and the trace of a matrix. The operator $\text{sign}(a)$ represents the sign of the real number a . For a complex number c , $\text{sign}(c) = \text{sign}(\Re(c)) + j\text{sign}(\Im(c))$, where $\Re(c)$ ($\Im(c)$) represents the real part of c (imaginary part of c). The operator $\text{sign}(\cdot)$ is applied element-wise to matrices. Consider a vector \mathbf{a} and a matrix \mathbf{A} , then $\text{diag}(\mathbf{a})$ and $\text{diag}(\mathbf{A})$ correspond to a diagonal matrix with diagonal entries equal to vector \mathbf{a} and a diagonal matrix with entries equal to the diagonal entries of the matrix \mathbf{A} , respectively. $\mathbf{A}(j,l)$ denotes the element at row j and column l of the matrix \mathbf{A} . \mathbf{I}_N is the identity matrix with size $N \times N$. The index u refers to the user terminal and p the receiver



Chapter 2

LTE-Advanced and Heterogeneous Networks

Mobile communications devices and broadband services have been increasing exponentially in the last decade. As such, recent mobile networks need to achieve high data rates and accommodate a large number of users. LTE-Advanced was introduced with the aim to solve that need. As part of LTE-Advanced, HetNets play a key role, as they are a flexible solution to cover high density populated and difficult covering areas.

This chapter starts by making an overview on LTE-Advanced. Then, the network architecture is presented, as well as the technologies employed in LTE-Advanced, such as multiple access techniques, carrier aggregation and heterogeneous networks.

2.1. LTE Advanced

As previously stated, LTE was developed by the 3GPP group. This technology has been introduced and enhanced through a number of releases. It started to be deployed commercially on release 8 as a candidate to 4G, even though it did not meet its requirements, set by the ITU-R. LTE-Advanced was introduced on release 10, this release was able to meet the stated 4G requirements. Currently the 3GPP group is on release 15.

LTE-Advanced, despite being an enhancement to LTE and introducing new technologies and techniques into the system, it is compatible with the already deployed LTE terminals. Some the technologies used on LTE-Advanced will be discussed further in this chapter.



2.1.1. Network Architecture

LTE brought a new core network architecture, known as System Architecture Evolution (SAE), which is simpler than its predecessor. This architecture, depicted in Figure 2.1, is comprised three main components, the User Equipment (UE), a new Radio Access Network (RAN), known as Evolved-Universal Terrestrial Radio Network (E-UTRAN) and a new core network, known as Evolved Packet Core (EPC).

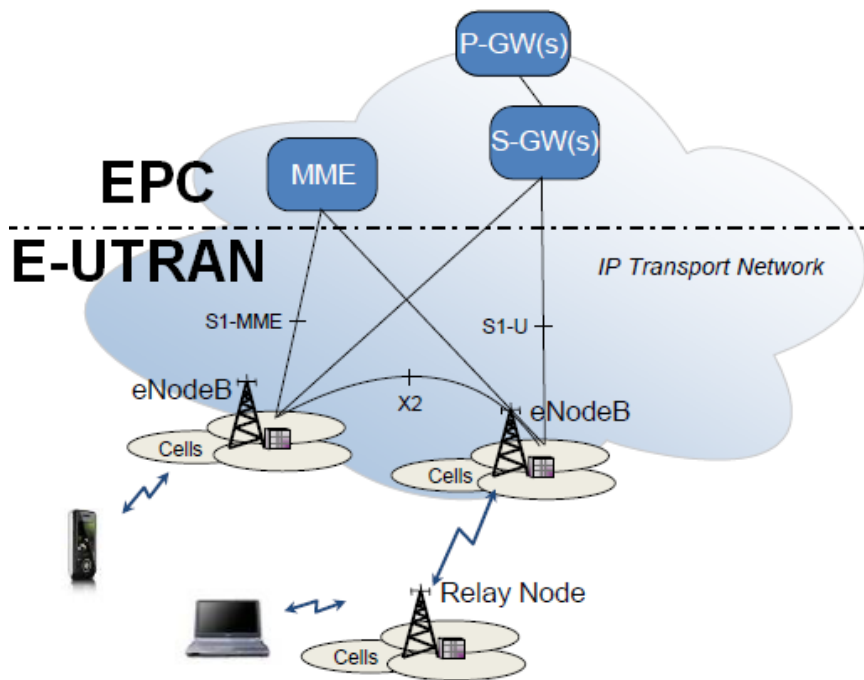


Figure 2.1. LTE-Advanced E-UTRAN and EPC architecture [31].

E-UTRAN

The E-UTRAN serves as the radio interface between the UE and the EPC. It is composed of evolved base stations, known as eNodeB, which connects to the EPC through an interface known as S1. These eNodeBs can further perform coding and decoding techniques, radio resource and mobility management and be connected with each other by an interface known as X2 to aid in the handover.



Evolved Packet Core

EPC is a full Internet Protocol (IP) core network architecture, designed to bring simplicity to the system, while maintaining compatibility with previous multiple access technologies. The EPC is composed by the following key elements:

- Mobility Management Entity (MME), which is the main control element in the EPC, since it handles the communications between the UE and core network. This element further handles the user mobility and security functions, such as authentication.
- Serving Gateway (S-GW), this gateway routes and forwards all the UE data packets to the P-GW and also along different LTE nodes to aid in the mobility.
- Packet Data Network Gateway (P-GW), which serves as the interface that communicates with the outside packet data networks.

2.1.2. LTE multiple access techniques

2.1.2.1. Downlink (OFDMA)

Orthogonal frequency-division multiple access (OFDMA) is a multiple access technique based on OFDM modulation, it can achieve high transmission data rates by splitting high data streams into multiple smaller data streams, which are simultaneously transmitted over different subcarriers spaced by 15kHz. This brings a lot of advantages [32], as the symbol time gets higher with the small data streams the Inter-Symbol interference (ISI) is reduced. Fading is also mitigated in a frequency selective channel, as the subcarriers are smaller the coherence band becomes apparently flat for each subcarrier. A higher spectral efficiency is also achieved without causing any inter-carrier interference (ICI) by overlapping orthogonal subcarriers, as seen in Figure 2.2.

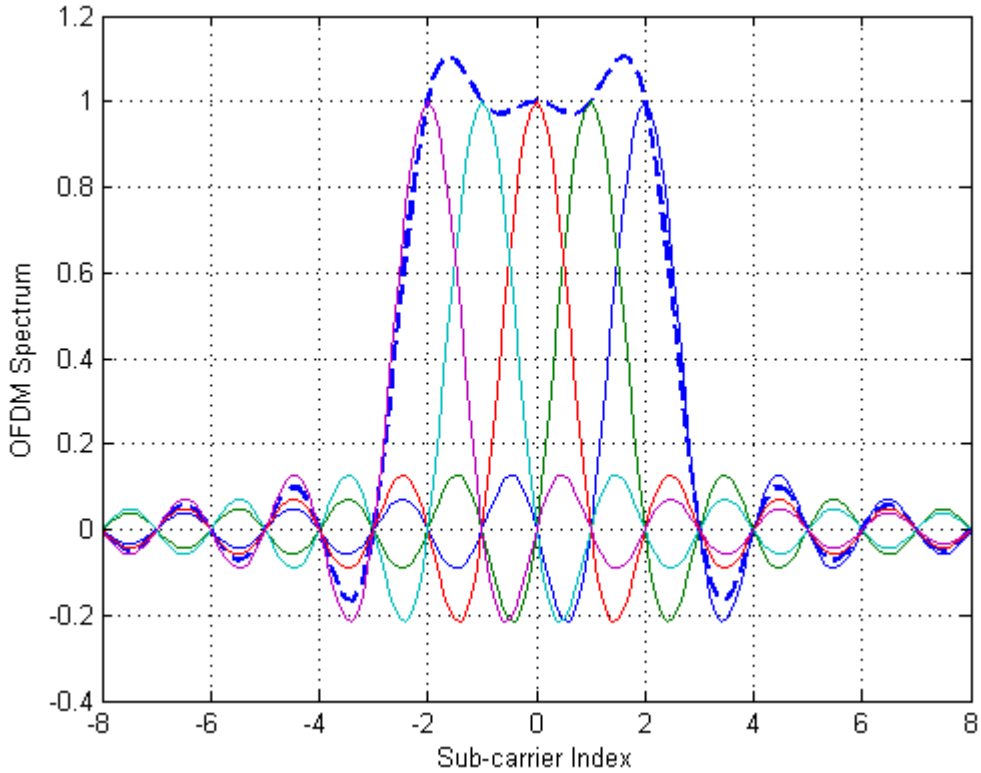


Figure 2.2. OFDM multiple sub-carriers and OFDM symbol [33]

Cyclic Prefix (CP)

Due to the negative effects of multipath, which increase the ISI, a CP is added to the data stream. This will mitigate the problem; however, it slightly reduces the spectral efficiency, a trade-off between both must be achieved.

As depicted in Figure 2.3, a CP with a guard time (T_G), chosen considering the multipaths' max delay, is added to the beginning of the data stream. This CP is built from the end of the data frame equivalent to the guard time.

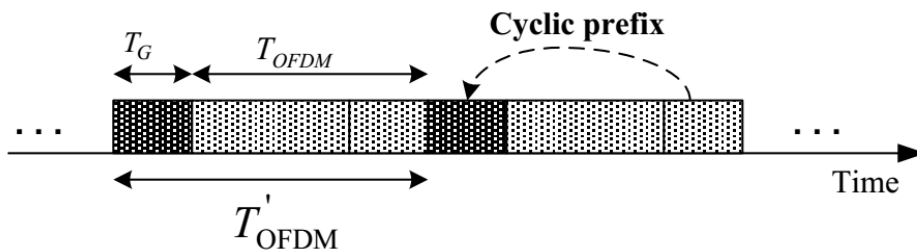


Figure 2.3. CP operation [34].



Frame Structure

In LTE, there are two types of frame structures. Type 1, for frequency FDD operation and type 2, for time division duplexing (TDD).

Type 1 is depicted in Figure 2.4. For this type, a LTE frame is 10 ms long in the time domain. This frame is subdivided in 10 Sub-Frames, each 1 ms long, where each Sub-Frame is further subdivided in 2 slots, 0.5 ms long each, resulting in 20 slots per frame. Each slot is built from 6 to 7 OFDM symbols, depending on whether the CP is short or long, respectively.

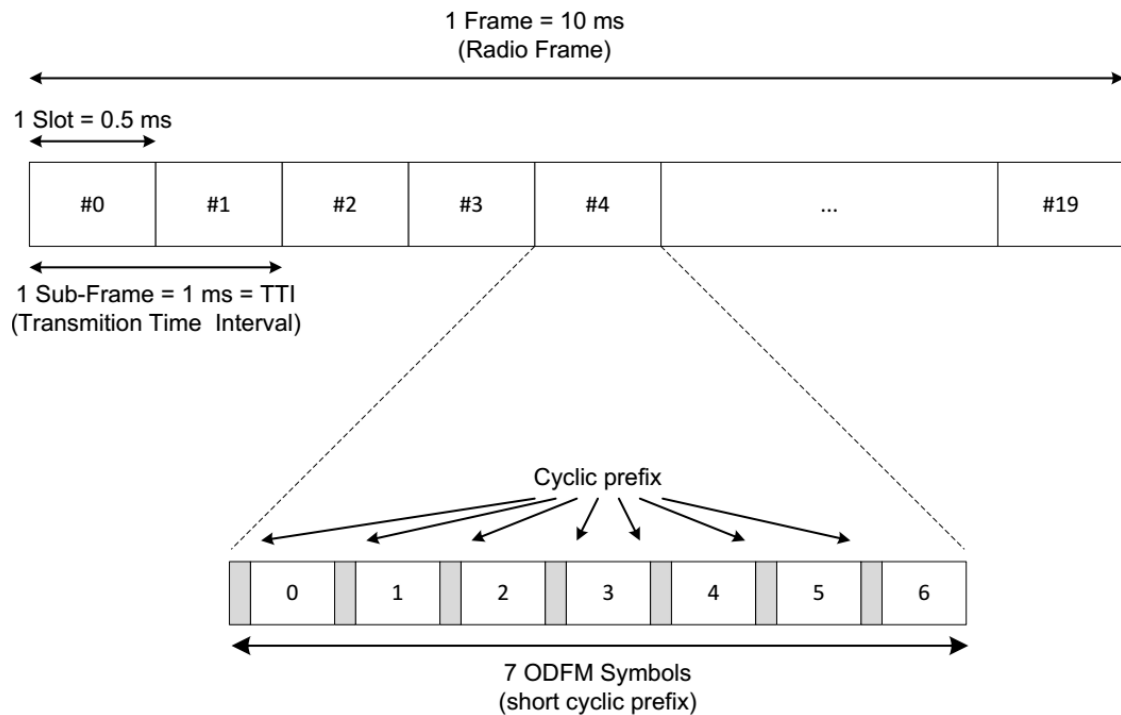


Figure 2.4. FDD LTE frame structure [34].

As for type 2, which is depicted in Figure 2.5, it also has a 10 ms long frame. This frame is subdivided in 2 half frames, 5 ms long each, which is further subdivided in 10 Sub-Frames, each 1 ms long. Apart from the standard Sub-Frames, half-frames also have 2 special Sub-Frames, which are made of 3 different fields. The downlink pilot time slot (DwPTS), uplink pilot time slot (UpPTS) and guard period (GP).

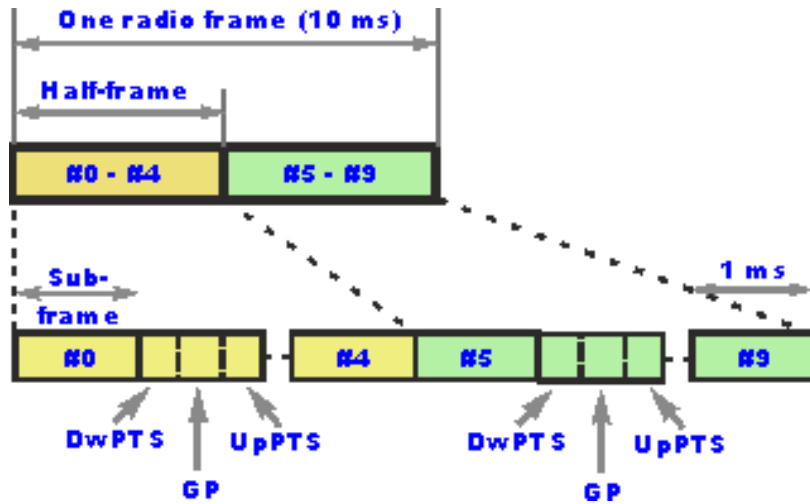


Figure 2.5. TDD LTE frame structure [35].

Resource Block

A resource block represents the smallest unit of resources to be assigned to the UE. These blocks consist of 12 subcarriers, with 180 KHz bandwidth and 1 slot long in time. The amount of transmitted resource blocks in a slot time, depending on the LTE system’s bandwidth can be seen on TABLE 2.I. While a representation of a resource block can be seen in Figure 2.6.

TABLE 2.I
LTE supported bandwidths [36]

Bandwidth	Resource Blocks	Subcarriers
1.4 MHz	6	73
3.0 MHz	15	181
5.0 MHz	25	301
10.0 MHz	50	601
15.0 MHz	75	901
20.0 MHz	100	1201



**LTE FDD Frame
1.4 MHz, Normal CP**

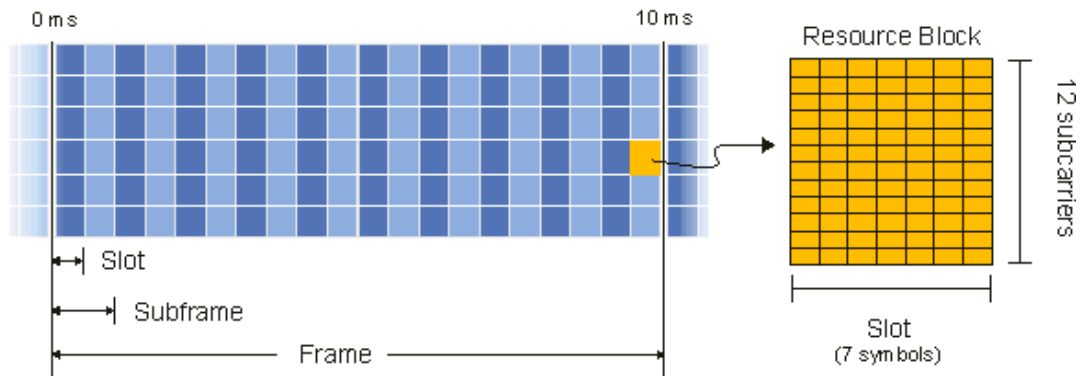


Figure 2.6. Resource Block with 1.4 MHz bandwidth and normal CP (short) [36].

2.1.2.2. Uplink (SC-FDMA)

Unfortunately, OFDMA has a high Peak-to-Average Power Ratio (PAPR) has a major impact on the power amplifiers efficiency, leading to a high energy consumption, which makes it unsuitable for the uplink, where the UE are powered by batteries.

As a solution single carrier frequency division multiple access (SC-FDMA) was adopted, by distributing the energy of the symbols over the subcarriers, it comes as a solution to the PAPR problem [37], while maintaining the advantages of the OFDMA.

The SC-FDMA frame structure and resource block is very similar to the OFDMA. The main different is in the symbol transmission, where in the SC-FDMA case the symbol is spread over the subcarriers, while in the OFDMA the symbol is transmitted over one subcarrier. These differences in symbol transmission are depicted in Figure 2.7.

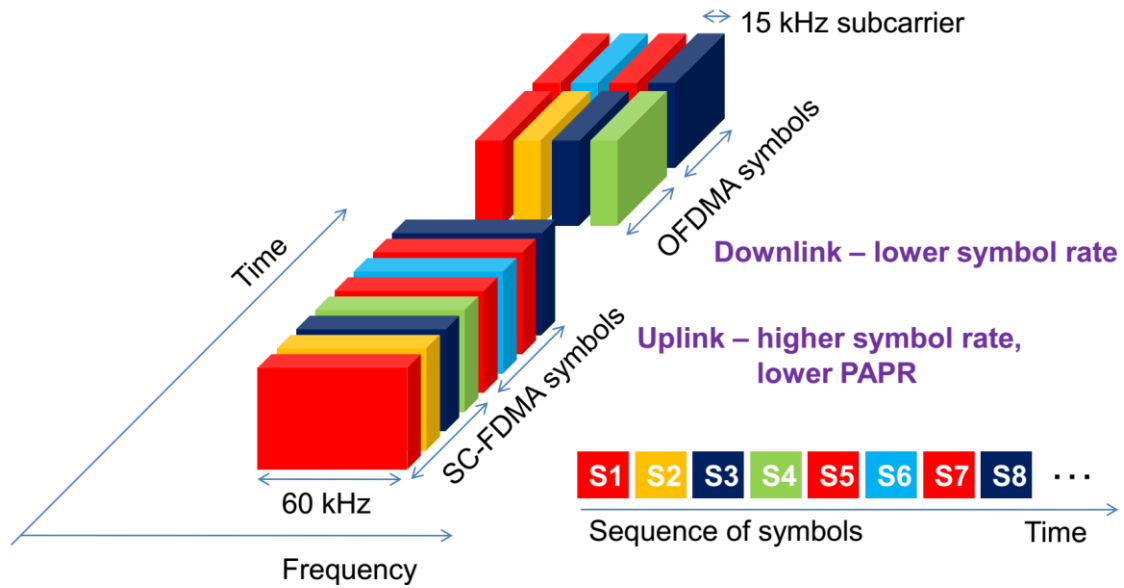


Figure 2.7. SC-FDMA and OFDMA data transmission [38].

2.1.3. Carrier Aggregation

LTE-Advanced introduced a new technique, carrier aggregation [39], which enabled it to meet some of the requirements set by ITU-R for 4G. This technique enables the increase system's bandwidth, without compromising the frequency spectrum restraints and keep backwards compatibility with older releases.

Due to the compatibility with the older releases, the bandwidth of each aggregated carrier is restrained by the ones of previous releases, see TABLE 2.I for the bandwidth values. It is possible to aggregate a maximum of 5 carriers, making it possible to achieve 100 MHz of bandwidth. While in TDD the number of aggregated carriers is normally the same for both upload and download, in FDD this number can differ. In this case, the number of aggregated carriers in the upload is always limited by the number in the download. An illustration of the operation in FDD can be seen in Figure 2.8.

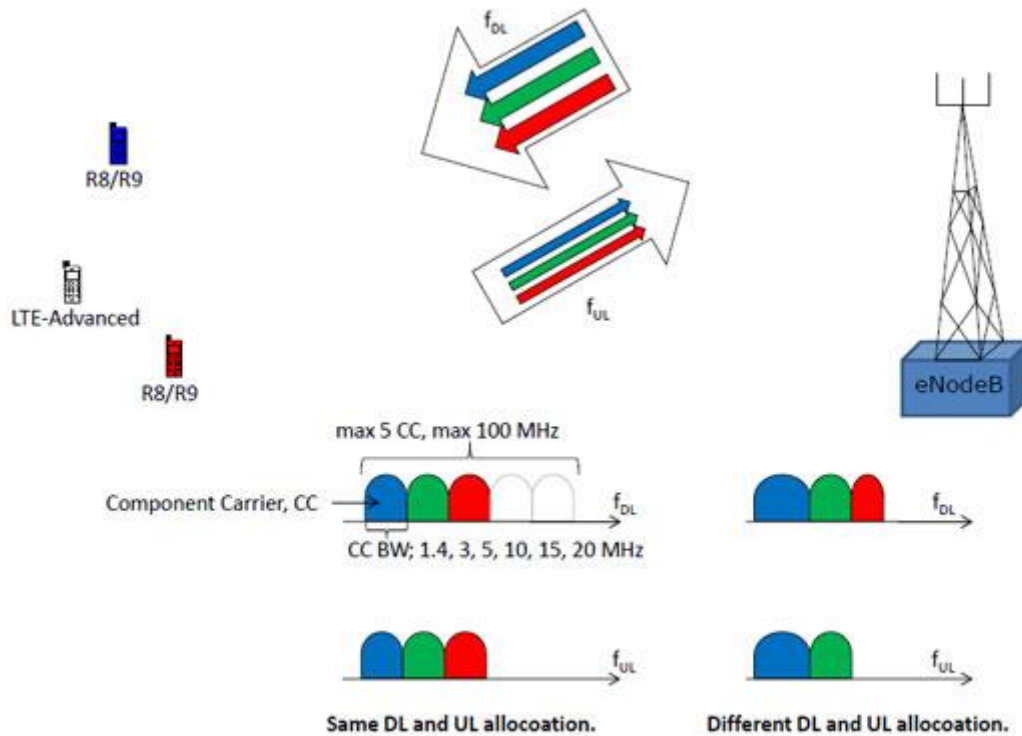


Figure 2.8. Carrier Aggregation in FDD [39].

2.1.4. MIMO Techniques

With a limited frequency spectrum for mobile communications, it is mandatory to achieve high spectral efficiency systems. However, it is hard to increase the system's capacity without decreasing its spectral efficiency. With MIMO technology, the data transmission medium is no longer restricted to time and space, as it explores space as a new dimension. MIMO systems are comprised of multiple antennas at both the receiver and transmitter, these systems are described in detail in Chapter 3.

LTE release 8 introduced the possibility to use on the downlink up to 4 antennas at both the receiver and transmitter (4x4 MIMO). However, no MIMO was introduced at the uplink. LTE-Advanced, pushed the technology forward and at release 10 introduced the possibility to use on the downlink up to 8 antennas at both the receiver and transmitter (8x8 MIMO) and at the uplink up to 4 antennas at both the transmitter and receiver (4x4 MIMO) [40].

2.1.5. Coordinated Multipoint (CoMP)

As an UE gets closer to the BS, Signal to noise Ratio (SNR) values increase and high data rates are easily achievable. However, as it gets closer to the cell-edge, the signal strength decreases, due to the distance, and interference increases, due to the neighboring cells, as such SNR values decrease and high data rates are harder to achieve.

CoMP is a technique introduced in release 11, used for both uplink and downlink with the purpose to address the aforementioned problem, improving the cell-edge network performance [40]. This technique can be applied for both homogeneous and heterogeneous networks.

There are two possible implementations for CoMP, an autonomous distributed/decentralized approach or a centralized approach, both depicted in Figure 2.9.

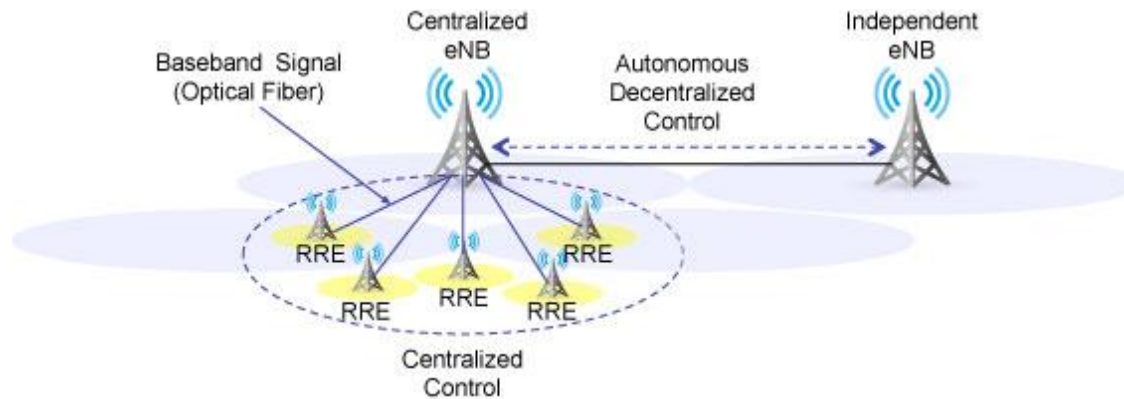


Figure 2.9. CoMP Centralized/Decentralized Control [41].

In the first decentralized method, independent EnodeBs communicate between each other in order to be coordinated. However, this method comes with signaling delays and overheads.

As for the second method, the centralized control is based on remote radio equipment (RRE), which are connected through optical fiber to the EnodeBs. In this scenario, the EnodeB performs the signal processing and control. As such, it needs to be able to process lots of data, which increases with the number of RRE. On the other hand, the signaling delay and overhead problem of the decentralized method is greatly reduced [42].

The CoMP operation is separated in downlink and uplink, as the processes are independent.



Downlink

At the Downlink, CoMP transmission can be done with two different schemes, as seen in Figure 2.10, joint processing and coordinated scheduling/coordinated beamforming. As for joint processing, it can be subdivided in two categories, joint transmission and dynamic cell selection. At joint transmission, the data is sent simultaneously to a single UE through multiple transmitters. This will increase the SNR of the signal at the receiver, making it possible to achieve higher data rates. Joint transmission can either be coherent or non-coherent. Coherent joint transmission, implies that the transmitters are synchronized when sending data. While in the non-coherent, the transmitters are not synchronized. This type of scheme requires a low latency for good coordination and a high bandwidth backhaul. At the dynamic cell selection, the data as to be available at multiple transmitters, while the UE selects the one with the best signal.

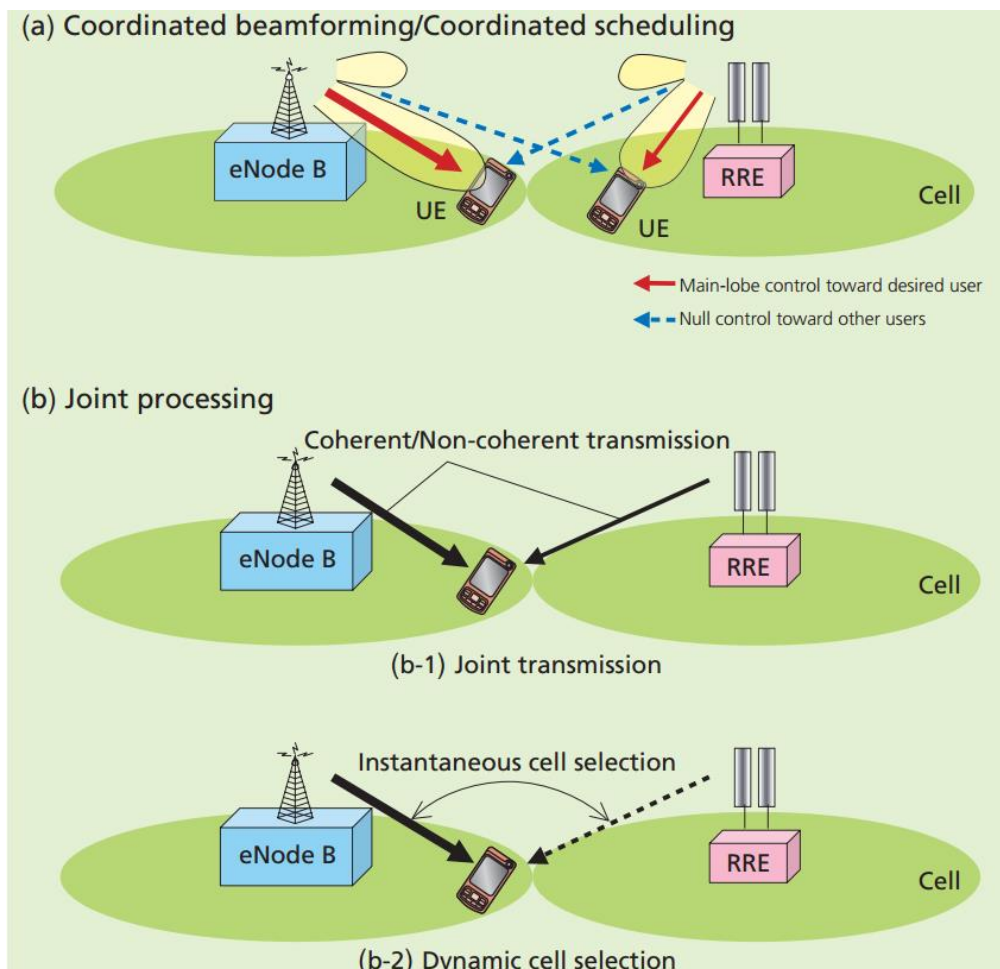


Figure 2.10. Downlink CoMP transmission [42].



At the coordinated scheduling/coordinated beamforming scheme, the data is sent from a single transmitter through beamforming techniques. These beams are then coordinated with other transmitters, so that interference can be avoided. This method reduced the backhaul bandwidth, as only coordination is needed and the data only needs to be at one transmitter.

Uplink

At the uplink, the UE does not need any knowledge of the neighboring receivers, as the signal is transmitted, as if just for one receiver. That signal is then captured by all neighboring receivers and combined.

2.2. Heterogeneous Networks

Traditional wireless systems were and are deployed in some sort of an “homogeneous” way. A high-power base station is deployed to cover a specific area, known as macro-cell, with regards to the physical characteristics of the area and the number of users. To avoid intercell interference, different frequency bands are used between cells, but due to frequency spectrum limitations, a certain frequency re-use is used, as depicted in Figure 2.11. However, this kind of networks lack flexibility. With an increase in traffic, the cell needs to be split in order to serve all users and avoid the system’s performance degradation. This process is costly, complex and time consuming.

A way to create flexibility, as well as increase the system’s performance and coverage is to “densify” the existing macro-cell, by introducing small-cells. The small cells are low-power nodes with different categories [43], [44], see TABLE 2.II, which allow to offload some traffic of the macro-cell or cover difficult areas. An example of a heterogeneous network can be seen in Figure 2.12, where different types of small-cells are used.

2.2.1. Possible Deployment Scenarios

As stated in [46], there are three possible deployment scenarios for HetNets.

- Multicarrier deployment, in which the small-cells use different frequencies than the macro-cell to avoid intercell interference. This method is undesirable due to its frequency spectrum inefficiency, as at least two different carrier frequencies are needed.



- Carrier aggregation deployment, where one carrier frequency is attributed solely to the macro-cell, while another carrier frequency is shared between both the macro and small-cells. However, this kind of deployment does not fare well in limited/small bandwidth systems.
- Co-channel deployment, in this scenario the macro and small-cells share the same frequency, which makes it the best choice for limited bandwidth systems. However, special care is required in the network deployment and interference coordination techniques may be needed. This type of deployment is the one considered in the work developed for this dissertation.

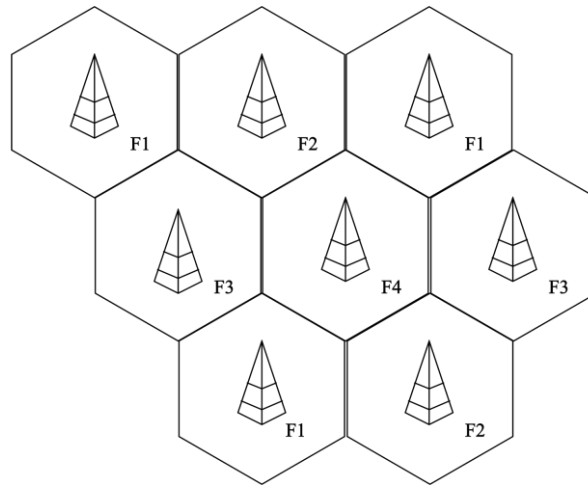


Figure 2.11. Traditional network deployment with frequency re-use [45].

TABLE 2.II
Small-cell types.

Nodes	Tx power	Coverage	Backhaul	Applications
Microcell	2W–20W	250m-1km	X2	Outdoors
Picocell	250mW–2W	100m-300m	X2	Indoors and Outdoors
Femtocell	10mW-200mW	10-50m	Internet IP	Indoors
Relay	1W	300m	Air-Interface	Outdoors

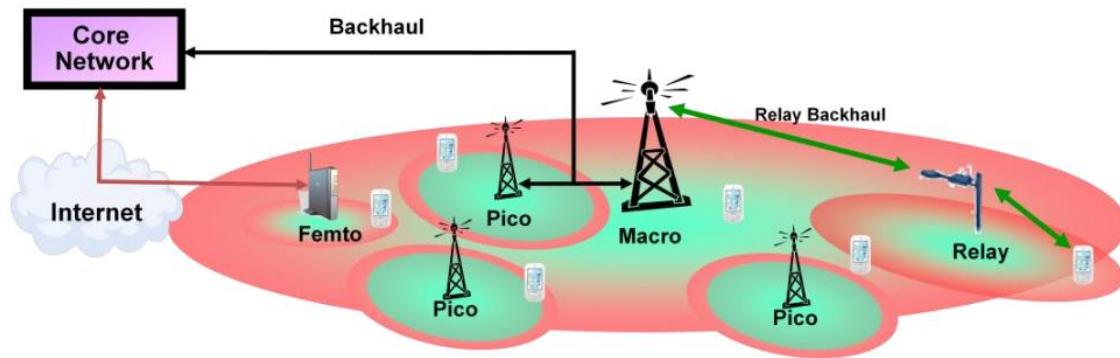


Figure 2.12. Example of a Heterogeneous Network.



Chapter 3

MIMO Systems

Multiple antennas can be deployed at both the transmitter and receiver, or as known in the mobile communications field, at the Access Point (AP) and UE, referred as MIMO systems. This increases the number of spatial dimensions, which can be exploited to increase the system's diversity and/or capacity. Instead of increasing the data rate for a single user (SU-MIMO), it is possible to serve multiple users (MU-MIMO). MIMO technology was introduced on LTE for mobile wireless communication. However, due to its potential, it is also used for Wi-Fi and other wireless systems.

This chapter starts by presenting the possible multi-antenna configuration. Then, the diversity and multiplexing concepts are explained, as well as the techniques on how to apply them to multi-antenna systems.

3.1. Multi-antenna types

With the possibility to deploy multiple antennas at the receiver and transmitter, 4 types of configurations can be achieved. For these configurations let's consider a system where the transmitter has L transmitting antennas and the receiver M receiving antennas.

3.1.1. SISO System

Single-Input-Single-Output (SISO) system refers to the typical radio system, where both transmitter and receiver are equipped with one antenna, as depicted in Figure 3.1. This kind of system does not introduce any extra spatial dimension, as such, assuming a



system without fading and with average white Gaussian noise, the system capacity is limited by the Shannon-Hartley theorem [47], with

$$C = B \log_2 \left(1 + \frac{S}{N} \right), \quad (1)$$

where, C is the system's capacity, B the bandwidth of the system, S and N the power of the signal and noise, respectively.



Figure 3.1. SISO system.

3.1.2. SIMO System

In a Single-Input-Multiple-Output (SIMO) system, the receiver is equipped with multiple M antennas, while the transmitter is equipped with a single antenna, as depicted in Figure 3.2. This kind of configuration is able to receive a signal from M different paths, increasing the system's diversity, this allows the system to be more robust to harmful channel propagation characteristics. However, it requires some processing at the receiver, increasing the complexity of the system, as well as an increase in power consumption and physical space, which can be a great disadvantage for small/mobile receiver devices.

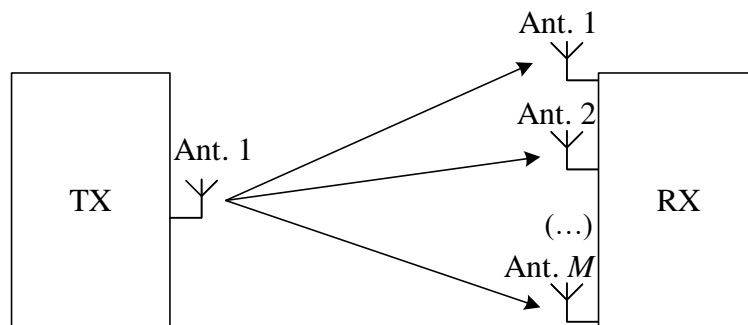


Figure 3.2. SIMO system.

3.1.3. MISO System

Multiple-Input-Single-Output (MISO) systems are similar to SIMO systems. In this case, the transmitter is equipped with L transmitting antennas, while the receiver is equipped with a single antenna, as depicted in Figure 3.3. These multiple antennas transmit the same data through different paths, increasing the system's diversity, which



makes the systems more robust to harmful channel propagation characteristics. For some applications, this configuration can be preferred to SIMO, as it moves some of the early stated SIMO disadvantages to the transmitter.

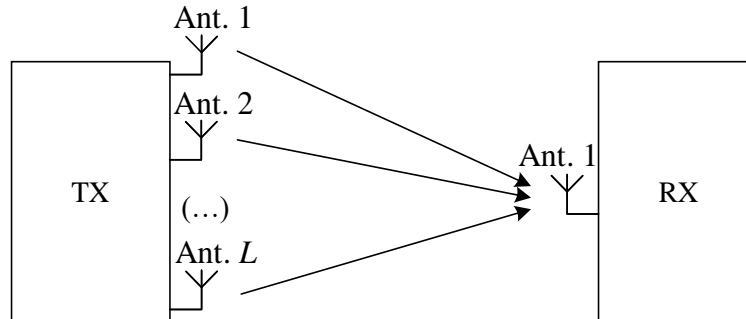


Figure 3.3. MISO system.

3.1.4. MIMO System

In the MIMO system, both the receiver and transmitter are equipped with multiple antennas, as depicted in Figure 3.4. As aforementioned, this type of configuration can increase both the system's diversity and capacity, by introducing spatial multiplexing. However, it requires some coding techniques at the transmitter and receiver, which increases the system's complexity.

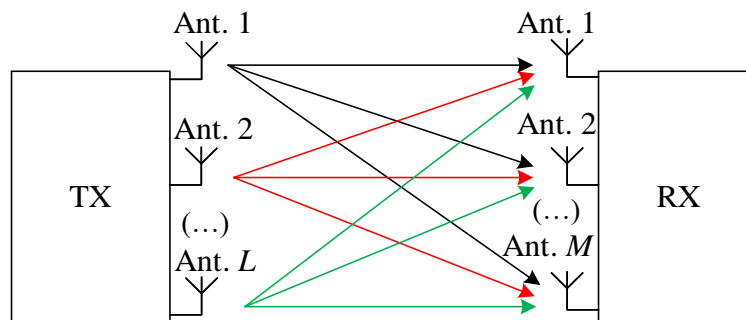


Figure 3.4. MIMO system.

3.2. Diversity

Diversity in communication systems can be achieved by introducing some redundancy in the system. This implies that the same information needs to be sent multiple times. A way to do it is by transmitting the same data through independent fading channels. This independency is achieved by having low or no correlation between channels. In this way, as the channels affect differently the same transmitted data, the

chances of having an error-free transmission, increases with the number of independent fading channels.

There are three different types of diversity:

- Time diversity, where diversity is achieved by sending the same data in slots separated with a time greater than the coherence time of the channel. However, this method decreases the data rate, with a factor equal to its number of repetitions.
- Frequency diversity, in which the same data is sent through different frequencies, that must be spaced at least by the coherence bandwidth of the channel [48]. Unfortunately, the system requires more bandwidth to apply it, which may not be ideal in an already limited spectrum.
- Spatial diversity, where multiple antennas create multiple independent fading channels, with the right spacing between the antennas [49]. In this method, there is no need to sacrifice either data rates or bandwidth.

3.2.1. Receive Diversity

Receive diversity is achieved when the receiver is equipped with multiple antennas, as the SIMO case. Any of the three types of diversity can be applied and, due to the multiple antennas, it is possible to achieve both diversity and antenna gain. Assuming that the transmitter has one antenna and the receiver is equipped with M antennas, as depicted in Figure 3.5, and all M channel propagation paths are independent, the diversity gain is given by the number of independent paths created, which in this case is the same as the number of antennas.

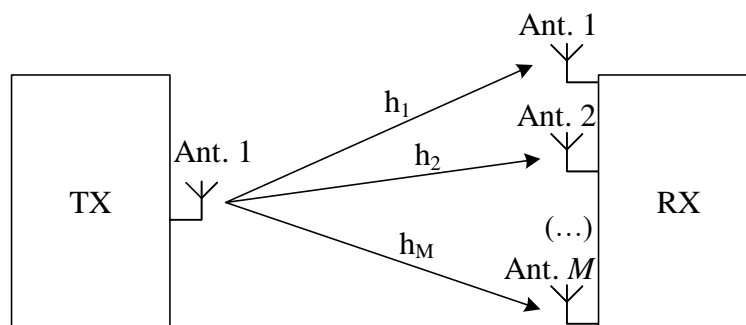


Figure 3.5. SIMO Receive Diversity

For the receiver to achieve the diversity gain, the received signals need to be combined. There are various combining methods, each with its complexity and needs,

such as Channel State Information (CSI). Where each have different performances when achieving diversity.

Equal Gain Combining (EGC) and Selection Combining (SC) are two possible low complexity methods, which do not require any CSI.

In SC, the received signals are compared, and the one with better SNR is chosen [50]. As for EGC and maximal ratio combining (MRC), they are linear combining methods, where the later requires CSI [49]. In these methods, the signals are added together. From these 3, MRC comes as the optimal solution, as it can maximize the received SNR.

3.2.2. Transmit Diversity

Transmit diversity is achieved when the transmitter is equipped with multiple antennas, as in the MISO case. Any of the three types of diversity can be applied due to the multiple antennas. However, in the case of transmit diversity, the data symbols cannot be sent simultaneously. This is due to the transmitted signals being added at the receiving antenna. Consider the scenario in Figure 3.6, a MISO system with the transmitter equipped with L antennas. By transmitting the same data simultaneously over the L antennas, the receiving antenna will add the signals and data will be seen as if it had only gone through one channel, which is the sum of all L channels instead of L independent channels. This results in no diversity in the system. To solve this problem some precoding techniques at the transmitter are needed. There are two main types of precoding techniques for transmit diversity, open loop and closed loop. The open loop techniques do not require the CSI to be known at the transmitter side. On the other hand, the closed loop techniques do require some knowledge of the CSI at the transmitter side.

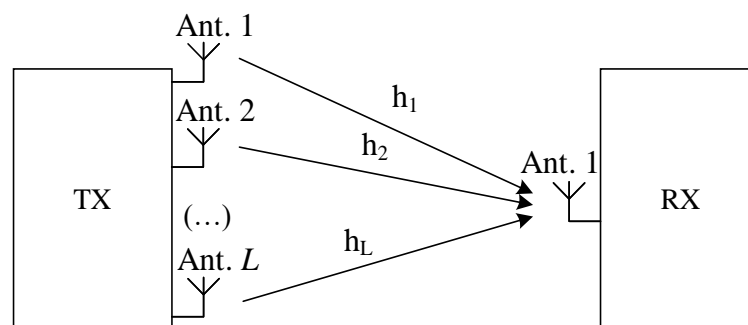


Figure 3.6. MISO transmit diversity.



3.2.2.1. Open Loop Techniques

As a way to achieve diversity, the same symbols can be sent at different times at different antennas, as opposed to the aforementioned scenario. An efficient way to do it is through space time/frequency coding techniques such as:

- Space time/frequency block coding (STBC or SFBC), with simple coding techniques. Where the Alamouti scheme is used for systems with 2 transmitting antennas and Tarokh codes for systems with more than two transmitting antennas;
- Space-Time Trellis Code, which, apart from the diversity gains, also introduce coding gain. However, unlike STBC these techniques are more complex;
- Layered Space-Time Codes, where the main focus is to boost multiplexing gain instead of diversity;

As the one used in LTE, only Alamouti scheme will be further discussed.

Alamouti schemes

In the Alamouti schemes the codes used in both transmitting antennas must be orthogonal between each other. This creates the possibility to use two different codes, however, only the one used in LTE system will be further discussed, which is described in TABLE 3.I.

TABLE 3.I
Alamouti code 1 (LTE)

Time/frequency	Antenna 1	Antenna 2
n	S_n	$-S_{n+1}^*$
$n+1$	S_{n+1}	S_n^*

Consider the MISO system scenario depicted in Figure 3.7, received signal is given by

$$\begin{bmatrix} y_n \\ y_{n+1}^* \end{bmatrix} = \begin{bmatrix} h_1 & -h_{n+1}^* \\ h_2 & h_n^* \end{bmatrix} \begin{bmatrix} s_n \\ s_{n+1} \end{bmatrix} + \begin{bmatrix} n_n \\ n_{n+1}^* \end{bmatrix}. \quad (2)$$

$\mathbf{y} \qquad \mathbf{H}_{eq} \qquad \mathbf{s} \qquad \mathbf{n}$

By soft decision, the estimated received symbols are given by

$$\hat{\mathbf{s}} = \mathbf{H}_{eq}^H \mathbf{y}, \quad (3)$$

which results in

$$\begin{bmatrix} \hat{s}_n \\ \hat{s}_{n+1} \end{bmatrix} = \begin{bmatrix} (|h_1|^2 + |h_2|^2) & 0 \\ 0 & (|h_1|^2 + |h_2|^2) \end{bmatrix} \begin{bmatrix} s_n \\ s_{n+1} \end{bmatrix} + \mathbf{H}_{eq}^H \mathbf{n}, \quad (4)$$

where a diagonal matrix is achieved, being equivalent to two different independent channels, achieving diversity.

For a system with more than one receiving antenna, this process can be replicated for each receiving antenna.

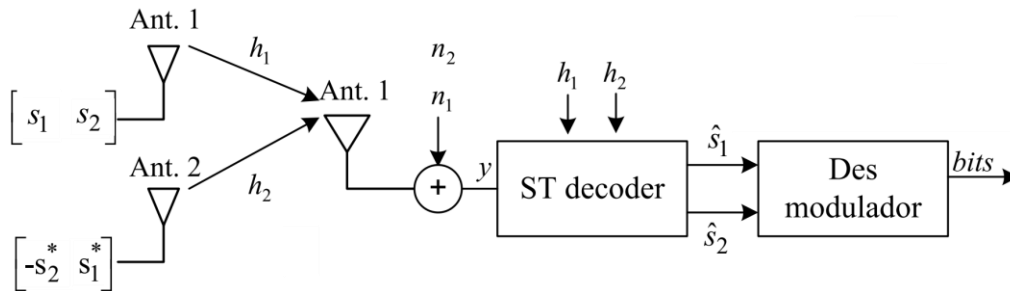


Figure 3.7. Block Diagram of the Alamouti space-time decoder [51].

3.2.2.2. Closed Loop Techniques

Closed loop techniques achieve diversity by applying beamforming and precoding techniques with some CSI knowledge, which, depending on the system's operation, can be fed back through different techniques.

In TDD systems there is channel reciprocity since the same frequency is used for both downlink and uplink. This makes it easier to be estimated, as the channel between the transmitter and receiver is the same.

In FDD systems, the channel has to be estimated in the receiver and fed back to the transmitter, as the downlink and uplink operate at different frequencies.

3.3. Spatial Multiplexing

To make it possible to apply spatial multiplexing techniques, multiple antennas must be equipped at both the transmitter and receiver. As such, it is not applicable to SISO, MISO and SIMO systems, where these system's capacity is limited by the Shannon-Hartley theorem, explained in (1). On the other hand, MIMO systems, through spatial multiplexing techniques can go beyond the aforementioned capacity limits. These techniques explore the degrees of freedom (DoF), which can be seen as possible parallel



links between transmitter and receiver. As such, they are limited by the minimum number of antennas at either the transmitter or receiver. In a system with L and M transmitting and receiving antennas, respectively, the number of DoF would be given by $\min(L, M)$ and further increase the system's capacity by that number, with no need for extra power or bandwidth. Depending on whether the channel is known just at the receiver, through a transmitted pilot signal, or at both the transmitter and receiver, the signal processing techniques differ.

3.3.1. Channel Known at the Transmitter

With the channel known at both the transmitter and receiver, through the decomposition of the channel matrix, using singular value decomposition (SVD), it is possible to convert the channel into a group of parallel channels [52].

Consider the system depicted in Figure 3.8, where the transmitter and receiver are equipped with L and M antennas, respectively. The received signal in a time-invariant channel is given by

$$\mathbf{y} = \mathbf{H}\mathbf{x} + \mathbf{n}, \quad (5)$$

where $\mathbf{y} \in \mathbb{C}^M$ denotes the received signal, $\mathbf{x} \in \mathbb{C}^L$ the transmitted signal, $\mathbf{n} \in \mathbb{C}^M$ the white Gaussian noise with variance σ^2 and $\mathbf{H} \in \mathbb{C}^{M \times L}$ the channel between the transmitter and receiver.

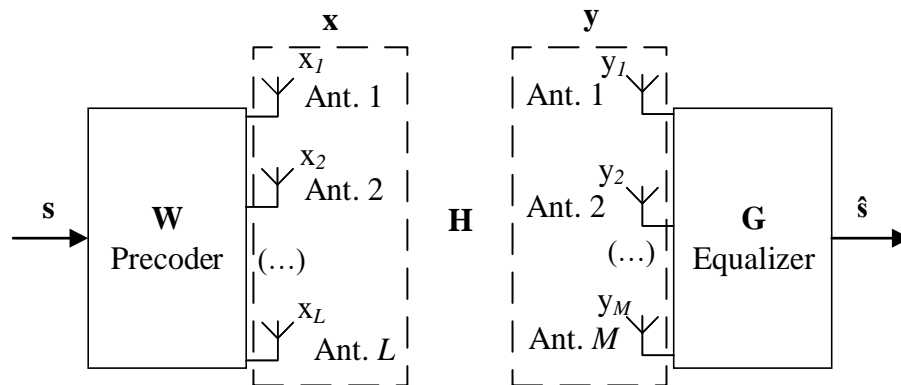


Figure 3.8. MIMO system.

Decomposing the channel matrix \mathbf{H} using SVD

$$\mathbf{H} = \mathbf{U}\mathbf{D}\mathbf{V}^H, \quad (6)$$

where $\mathbf{U} \in \mathbb{C}^{M \times r}$ and $\mathbf{V} \in \mathbb{C}^{L \times r}$ are unitary matrices and $\mathbf{D} \in \mathbb{R}^{r \times r}$ is a diagonal matrix



with non-negative real numbers. The diagonal elements of the matrix $\mathbf{D} (\lambda_1, \lambda_2, \dots, \lambda_r)$ are the singular values of the matrix \mathbf{H} , such that $r = \text{rank}(\mathbf{H}) \leq \min(L, M)$.

The precoder matrix \mathbf{W} is given by

$$\mathbf{W} = \mathbf{V}\mathbf{P}^{1/2}, \quad (7)$$

where $\mathbf{W} \in \mathbb{R}^{L \times r}$ and $\mathbf{P} \in \mathbb{R}^{r \times r}$ is a diagonal power allocation matrix. As for the equalizer \mathbf{G} , it is given by

$$\mathbf{G} = \mathbf{U}^H, \quad (8)$$

where $\mathbf{G} \in \mathbb{R}^{r \times M}$.

The transmitted signal is then

$$\mathbf{x} = \mathbf{W}\mathbf{s}, \quad (9)$$

where $\mathbf{s} \in \mathbb{R}^{r \times 1}$ is the vector of r symbols to be sent in parallel. With this, the received signal given in (5) becomes

$$\mathbf{y} = \mathbf{U}\mathbf{D}\mathbf{V}^H \mathbf{V}\mathbf{P}^{1/2}\mathbf{s} + \mathbf{n}. \quad (10)$$

As for the estimated symbols $\hat{\mathbf{s}}$, they are given by

$$\hat{\mathbf{s}} = \mathbf{G}\mathbf{y} = \mathbf{U}^H \mathbf{U}\mathbf{D}\mathbf{V}^H \mathbf{V}\mathbf{P}^{1/2}\mathbf{s} + \mathbf{U}^H \mathbf{n} = \mathbf{D}\mathbf{P}^{1/2}\mathbf{s} + \tilde{\mathbf{n}}. \quad (11)$$

Resulting in an ISI free transmitted symbols. As for the power allocation, as the channel is known, the water filling method is used [53]. In this method, the channels with the worst characteristics, above a certain threshold, are discarded, and the power is distributed over the other channels.

3.3.2. Channel Not Known at the Transmitter

With the channel only known at the receiver, it is possible to achieve the same data rate as the previous case. However, the complexity of the receiver's architecture greatly increases with the number of transmitted symbols. For that, simple sub-optimal linear receiver architectures are used.

3.3.2.1. Zero Forcing (ZF)

The ZF equalizer is designed to remove the channel component from the signal, consequently removing the ISI. This is done by applying the inverse of the channel frequency response to the received signal [54]. With this, the equalizer is given by



$$\mathbf{G}_{ZF} = (\mathbf{H}^H \mathbf{H})^{-1} \mathbf{H}^H . \quad (12)$$

However, the performance is greatly reduced in the presence of noise, low SNR, as the noise component is amplified by the equalizer.

3.3.2.2. Minimum Mean Square Error (MMSE)

MMSE equalizers try to reach a compromise between reducing the ISI and noise. As such the equalizer is given by

$$\mathbf{G}_{MSE} = (\mathbf{H}^H \mathbf{H} + \sigma^2 \mathbf{I}_M)^{-1} \mathbf{H}^H . \quad (13)$$

This makes it a better solution for low SNR application than the ZF. However, its performance at high SNR is similar to the ZF



Chapter 4

Massive MIMO with mmWave Communications

As discussed in the introduction, Massive MIMO and mmWave Communications are promising technologies to be employed in 5G. In this chapter, the individual benefits and limitations is covered. Then, the advantages of combining both these technologies is presented, as well as possible architectures to employ them.

4.1. Massive MIMO systems

With the arrival of 5G and the IoT, the demand for a greater capacity in a limited frequency spectrum will increase. Massive MIMO comes as a candidate technology to make these concepts feasible.

By making use of a massive number of antennas, in the hundreds, it allows the possibility of beamforming and consequently spatial multiplexing. This brings the possible scenario seen on Figure 4.1, where different devices are served by a different beam in the same time-frequency resource, differentiated in space (spatial multiplexing). Furthermore, multiple data streams can be transmitted to each of these served devices. This is a very important aspect, as the demand for frequency bands is high and the frequency spectrum is a limited resource and currently overloaded. Massive MIMO is also a scalable technology, where adding extra antennas into the system will improve its performance.

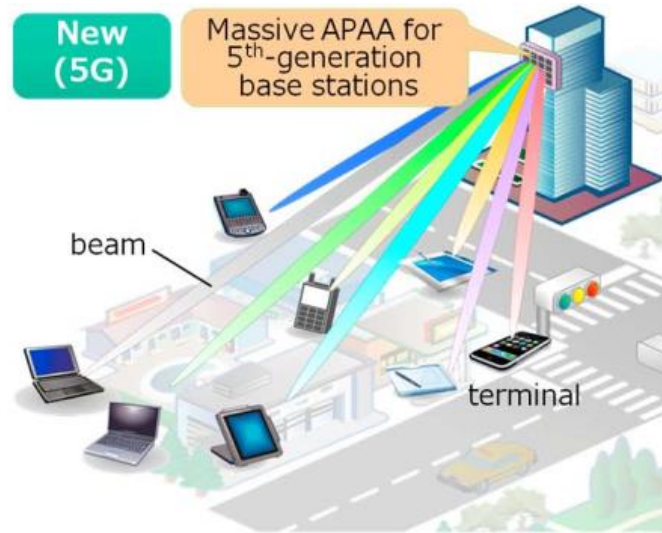


Figure 4.1. Example of massive MIMO operation [55].

As these massive MIMO systems employ a greater number of antennas, these systems can very easily reach high levels of complexity. As such, linear precoding and decoding techniques are good candidates to mitigate this problem due to their simplicity. Furthermore, as the number of antennas increase, the performance of these techniques approach the theoretical Shannon capacity limits [56].

In order to keep massive MIMO scalable, the estimated CSI should be measured instead of assumed [56], working over a closed loop. As such, some sort of feedback is required in the uplink, such as pilot sequences. Because of this, massive MIMO works preferably over TDD mode, but research is being made to make it efficiently work over FDD mode. This advantage of TDD over FDD, comes from the processing of the CSI, which is simplified in TDD operation, thanks to its channel reciprocity characteristic [57].

4.1.1. Benefits and Limitations of Massive MIMO

The benefits of massive MIMO in comparison with the current systems are quite appealing, some of these benefits are described below [12]:

- Increased capacity:
Capacity can be increased by 10 time or more, this comes from the possibility of spatial multiplexing stated earlier.
- Increased energy efficiency:
With the possibility of beamforming, energy can be focused onto the receiver.



This way the energy is not wasted on the sidelobes or propagating where there is no receiver.

- Increased spectrum efficiency:
By spatial multiplexing, a multitude of devices can be served in the same frequency.
- Lower latency:
By beamforming, the area of transmission is smaller, this brings less reflections and consequently a lower multipath fading.
- Inexpensive low-power components:
With a massive number of antennas, the power amplifiers (PA) require less power for each antenna. This also contributes for the energy efficiency, as the PAs are less efficient for higher amplifications.
- Increased robustness to jamming.
- Simplified Media Access Control (MAC) layer.

However, Massive MIMO has its limitations, as seen in [58], some of them are:

- Channel reciprocity, by working over TDD it requires channel reciprocity and the hardware chains may not be reciprocal over both the uplink and downlink.
- Pilot-contamination, due to the pilot re-use, because of the limited number of pilot sequences.
- Radio propagation and orthogonality of channel responses.

4.2. Millimeter Wave Communications

As stated earlier, the frequency spectrum is overloaded and has a high demand for its frequency bands. Going up in the frequency spectrum comes as an inevitable solution. MmWave band refers to both super high frequencies (3-30 GHz) extremely high frequencies (30-300 GHz) bands. As such, the 3-300 GHz band is attributed to the mmWave band, with wavelengths in the orders of millimeters (1-100mm) [59].

4.2.1. Benefits and Limitations of Millimeter Wave Communications

This new spectrum range brings several possible benefits to future communication applications. Some of these advantages are discussed below [11]:



- Spectrum availability, as stated before, the available spectrum will range from 3 to 300 GHz, where there are already some defined telecommunications bands [16].
- Limited range and beamwidth, this characteristic can be seen as an advantage or limitation. As an advantage, it brings an improvement to security and short-range communications.
- Reduced antenna size, with the increase in frequency, the physical size of the antennas is reduced. When working at such high frequencies the size of the antennas becomes really small, which will unlock new transmission techniques, as it is possible to fit a great number of antennas in small physical space.

Despite the benefits previously stated, high frequencies come with a set of drawbacks in their propagation characteristics, such as:

- Reduced coherence time, since it decreases as the Doppler spread increases [4], where the change in frequency due to the Doppler effect is given by [60]

$$\Delta f = \frac{\Delta v}{c} f_c, \quad (14)$$

where Δf is the frequency shift due to the Doppler effect, Δv the relative velocity between the source and the receptor and f_c the carrier frequency.

- Free-space propagation attenuation increases with the frequency, which can be seen by the Friis formula [61]

$$P_r = P_t + G_t + G_r + 20 \log \left(\frac{c}{4\pi R f_c} \right) [dBm], \quad (15)$$

where P_r is the receiving power, P_t the transmitted power, G_t the gain of the transmission antenna, G_r the gain of the receiving antenna, R the distance between the transmission and receiving antennas and f_c the carrier frequency.

- Shadowing, as the wavelength gets smaller, the penetration characteristics get weaker, this makes the transmission over walls difficult [62], which is particularly relevant when considering an urban environment.
- Atmospheric absorption, as it can be seen on Figure 4.2, despite having the whole mmWave frequency band, not all of it is equally good for propagation.



- Propagation in rain, the size of the rain droplets is also in the orders of millimeters. As such, they may cause scattering on the transmitted signals.

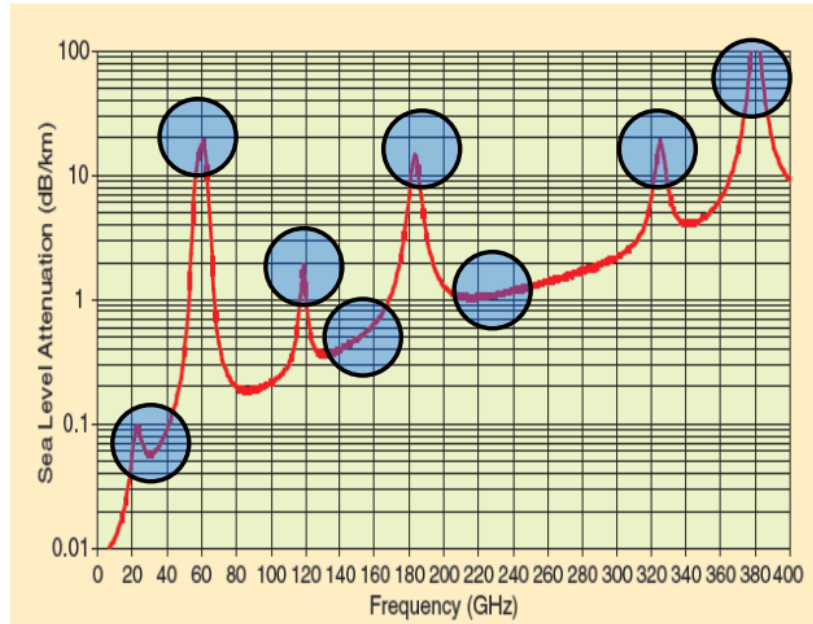


Figure 4.2. Atmospheric absorption [63].

4.2.2. Benefits of mmWave massive MIMO Systems

By joining massive MIMO with mmWave, the beamforming capability of massive MIMO when applied to mmWave mitigates some of the previously stated drawbacks, while maintaining its benefits. Some of these benefits are described below:

- Increased coherence time, with the beamforming capability of massive MIMO, the coherence time can be increased. As seen on Figure 4.3, the coherence time gets higher as the beamwidth gets narrower.
- Reduced free-space propagation attenuation. There is no apparent increase in the free-space attenuation, considering the same transmitted power and physical area [64]. Since the antennas are smaller, it is possible to place more of them in the same area of an antenna that operates at lower frequencies.

As for the shadowing, it gets worse since the transmission is confined to a beam. This beam can be easily blocked, because of the bad penetration characteristics of the mmWaves and the absence of alternate paths.

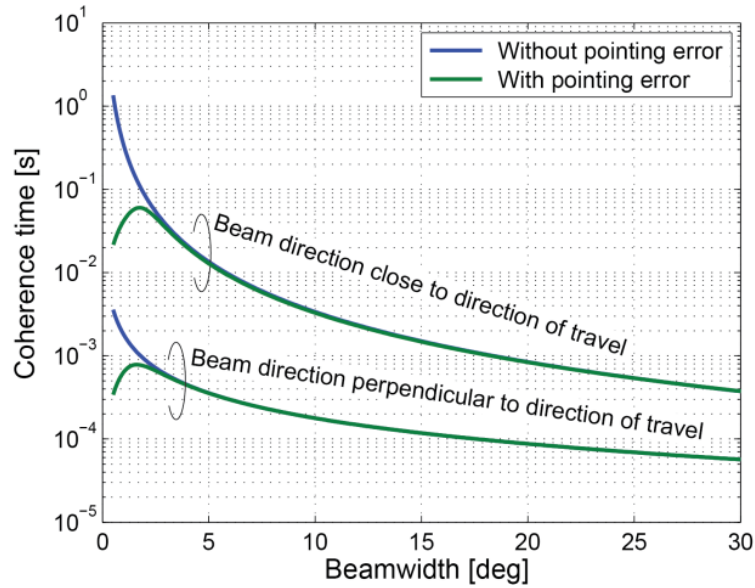


Figure 4.3. Variation of the coherence with the beamwidth [65].

4.2.3. Benefits of mmWave massive MIMO Systems in HetNets

As aforementioned, these technologies, mmWave communications, massive MIMO and HetNets, when deployed alone, each have their own limitations. However, they perfectly go together, besides the already discussed benefits of mmWave massive MIMO systems and HetNets, when employed together the capacity of the systems can increase in great orders and the shadowing effect that persisted is also solved to some degree [66]. An example of such system can be seen on Figure 4.4.

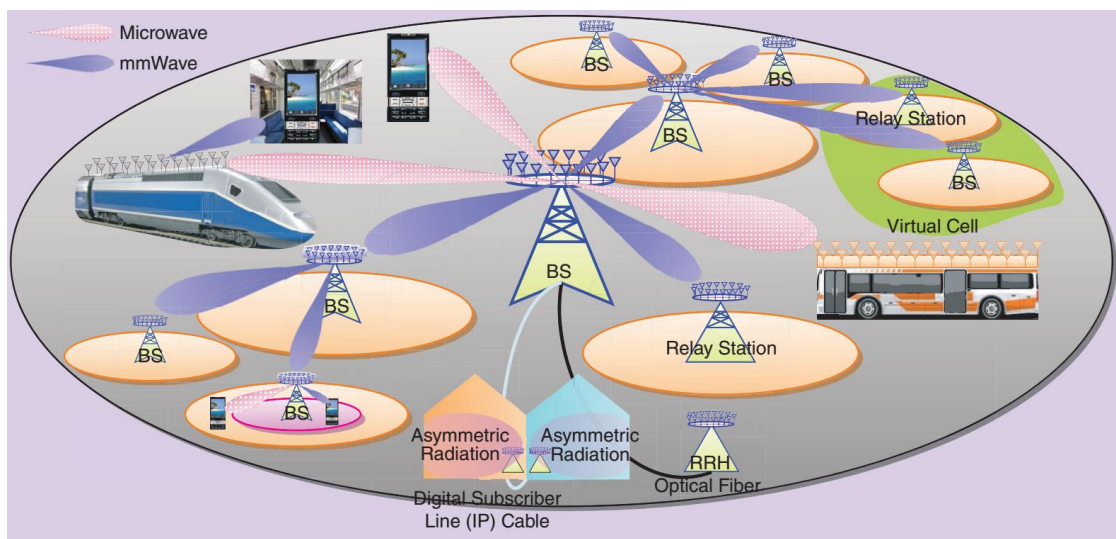


Figure 4.4. Possible mmWave massive MIMO HetNet system [66].

4.3. MmWave Massive MIMO Beamforming Architectures

As aforementioned, beamforming techniques play a crucial role in mmWave massive MIMO systems. As the high path losses at high frequencies can be bypassed by redirecting the energy into a beam. To achieve a beam, high antenna gains are needed at the desired direction. For that, control over the phase of the signal at each antenna at both the receiver and transmitter is needed. This arises several hardware constraints, as such, new architectures need to be researched where signal processing also plays a big role [67]. Three different beamforming schemes are possible, which will be discussed below, analog, digital and hybrid beamforming.

4.3.1. Digital Beamforming

As depicted in Figure 4.5, digital beamforming performs some digital precoding/combining at baseband and is comprised of as many DACs and RF chains as the number of antennas. As each DAC is connected to a RF chain which is connected to a single antenna. This type of architecture offers the possibility to transmit multiple data-streams and beams. Furthermore, if the CSI is known at the transmitter it is possible to achieve optimum transmission. However, it is not feasible due to hardware constraints. In mmWave massive MIMO systems the number of antennas is high and the spacing between them is small. As such, this architecture would greatly increase the system's cost and power consumption. Its physical implementation would be hard to achieve due to the size of the hardware.

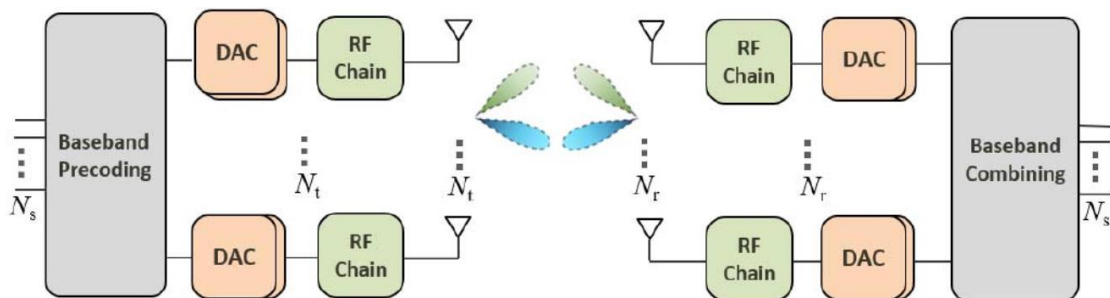


Figure 4.5. MmWave massive MIMO system using digital beamforming [67]

4.3.2. Analog Beamforming

From all of these architectures, analog beamforming is the most straightforward approach. As it can be seen on Figure 4.6, every antenna is connected to a digitally controlled phase shifter. Which makes it possible to redirect the beam to the desired direction. In addition to that, all of these phase shifters are connected to a single RF chain, limiting it to a single data stream. This type of beamforming is also limited to a single beam. Therefore, analog beamforming does not take advantage of multi-stream and multi-user modes, typical of MIMO technologies.

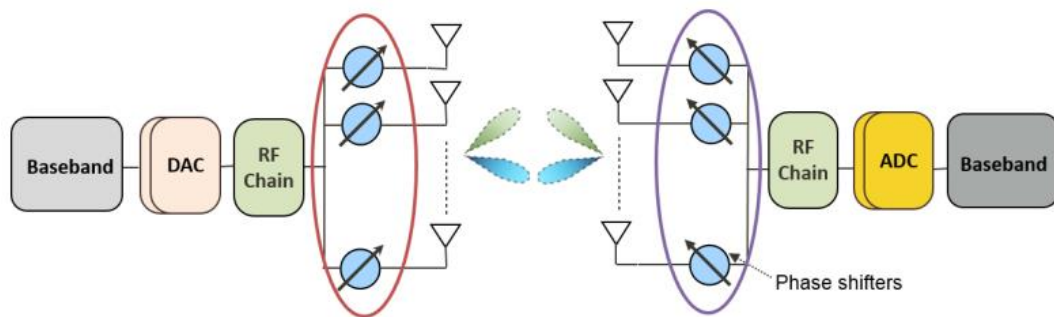


Figure 4.6. MmWave massive MIMO system using analog beamforming [67].

4.3.3. Hybrid Beamforming

Hybrid beamforming consists on a compromise of both analog and digital beamforming architectures. Therefore, a trade-off between the good performance of digital architectures and low hardware complexity of analog architectures is made. As depicted in Figure 4.7, this hybrid architecture is comprised of some baseband precoding/combining, with a number of DACs and RF chains (L_t) inferior to the number of antennas (N_t), as well as a RF precoding/combining stage, in charge of controlling the phase shifters. Therefore, multiplexing capabilities are added to the system and it is possible to achieve multiple data streams (N_s) and beams, in a way that $N_s \leq L_t$ and consequently serve up to N_s users.

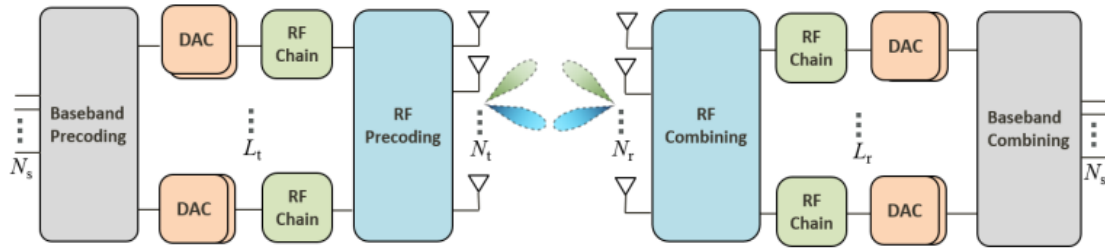


Figure 4.7. MmWave massive MIMO system based on hybrid analog-digital precoding and combining [67].

Regarding the RF precoding/combining blocks, there are different ways to implement them. Three of them are discussed below, by using phase shifters, switching networks and lenses.

4.3.3.1. Processing based on phase shifters

As depicted in Figure 4.8, there are two possible implementations on phase shifters in the analog domain. At (a) each RF chain is connected to every single antenna, while at (b) each RF chain is connected to a subset of antennas. The difference between both is that the one offers more flexibility and control, while the later a lower hardware complexity. As such, a compromise can be found with the size of the subset of antennas.

The implementation of this type of analog processing in hybrid architectures is advantageous, as the digital precoding part can correct any irregularity of the analog processing.

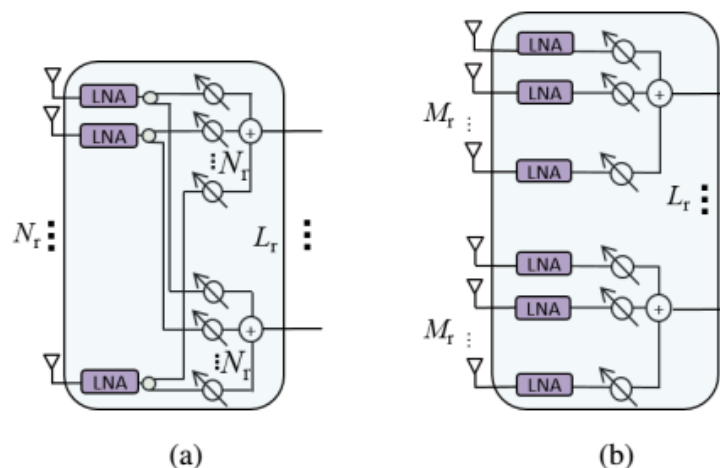


Figure 4.8. Analog processing for hybrid beamforming based on phase shifters [67]:
 (a) each RF chain is connected to all the antennas;
 (b) each RF chain is connected to a subset of antennas.

4.3.3.2. Processing based on switches

A less complex and power efficient alternative to phase shifters is the use of switching networks. In this method, at the receiver, a sampling process can be done without sacrificing the quality of the signal. As depicted in Figure 4.9, there are also two possible implementations for this type of processing. Like its phase shifters counterpart, in (a) each RF chain can switch through every antenna and in (b) each RF chain is connected to a subset of antennas. As such, a compromise should be met depending on the number of antennas and RF chains.

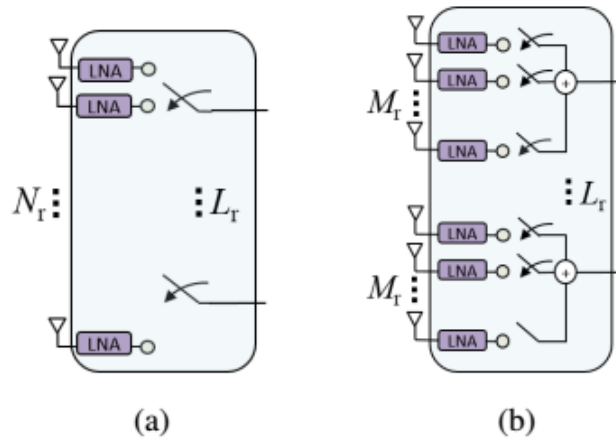


Figure 4.9. Analog processing for hybrid beamforming based on switches [67]:

- (a) Each RF chain can be connected to all antennas;
- (b) each RF chain can be connected to a subset of antennas.

4.3.3.3. Processing based on lenses

At the transmitter, it is also possible to use lenses to perform beamforming. By applying a continuous aperture phased (CAP) MIMO transceiver, as seen in Figure 4.10, it is possible to achieve a low complexity system, when compared to the other methods.

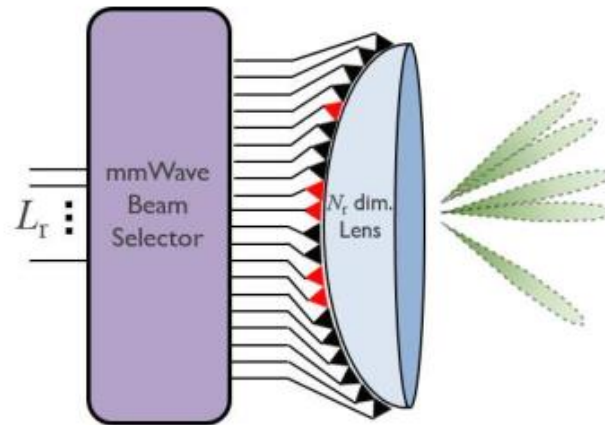


Figure 4.10. The CAP-MIMO transceiver that uses a lens-based front end for analog beamforming; it maps the $p=N_s$ precoded data streams to $L = O(+)$ beams via the mmWave beam selector and lens [67].



Chapter 5

Hybrid Beamforming Designs for Massive MIMO mmWave Heterogeneous Systems

Network densification through the deployment of small cells along the coverage area of a macro-cell, employing massive MIMO and mmWave technologies, is a key approach to enhancing the network capacity and coverage of future systems. For ultra-dense mmWave heterogeneous scenarios with a massive number of users, one should address both inter- and intra-tier interferences contrary to the low-density scenarios where the network is mainly noise-limited. Therefore, this chapter proposes low complex hybrid analog-digital receive and transmit beamforming techniques for ultra-dense uplink massive MIMO mmWave heterogeneous systems to efficiently mitigate these interferences.

For the design, the following considerations were taken:

- At the small cells, a distributed hybrid analog-digital architecture was considered, where the analog part is performed at the small cell base stations and the digital part at the central unit for joint processing. The main motivation to consider a distributed hybrid analog-digital processing at the small cells, is that the information to be sent by the access points to the central unit is significantly reduced, since the number of RF chains is much lower than the number of antennas. Moreover, the signals are transported through the front-haul in the analog domain.



- To efficiently cancel the inter-tier interference, the digital part of the precoders employed at the small cells user terminals are designed in a way that this interference resides in a low dimension at the macro base station. We show numerically that 2 bits of inter-tier information exchange are enough to efficiently align the inter-tier interference with a good overall network performance.
- To optimize the analog part of the hybrid equalizer and the precoders used at both the macro and small cell user terminals, we minimize the distance between the hybrid and fully digital approaches. In the optimization problem, we impose the constraints of the analog part and the constraints inherent to the distributed nature of the small cells access points. This approach is significantly different from the single tier case where the analog and digital parts are centralized and therefore, the optimization problem is less complex.

The chapter starts by introducing the system model, describing the scenario, both the receiver and transmitter architecture and the channel model. Then, various analog/digital precoders and equalizers are presented, as well as the proposed design.

5.1. System Model

Considering the uplink of a two-tiered network whose carrier frequency is in the mmWave band. The two-tiered network comprises a macro-cell with N small cells within its coverage area (all sharing the same frequency spectrum), as depicted in Figure 5.1. The macro-cell has a BS and one user terminal (UT). Each small cell has an AP which serves the UT. The APs have an analog-only architecture, i.e., the signals are processed in the analog domain. The processed analog domain signals are sent through a fiber-based front-haul network to a central unit (CU), where they are digitized and jointly processed in the digital domain. Namely, for the small cells, the analog and digital processing are distributed (the analog processing is done at the APs and the digital processing at the CU and for the macro-cell, the analog-digital processing is centralized at the BS).

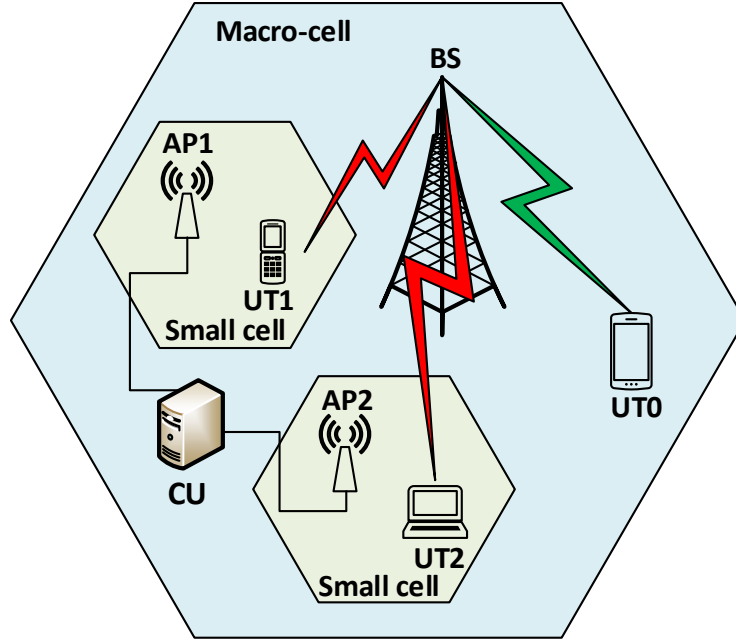


Figure 5.1. System model, example with 2 small cells within the macro-cell

At the receiver side, the small cells have two entities, the N APs, which perform the analog processing and a CU which performs the digital processing. In contrast, the macro-cell has just one entity, the BS, which performs both the analog and digital processing. To simplify the description, in the following sections the BS is divided into two logical entities, equivalent to the ones at the small cells, where the analog and digital processing occurs. With a slight abuse of terminology, it will be denominated by BS the logical entity performing the digital processing and will give a different name to the analog entity. Henceforth, to standardize the notation between the macro and small cells, the macro UT is denoted by UT_0 and the UT of the p^{th} small cell by UT_p . At the receiver side, the logical entity that performs the analog processing is denoted by RX_p , with $p \in \{0, \dots, N\}$. The digital domain entities are denoted by BS and CU, for the macro and small cells, respectively. From now on, it will be assumed that the UT_p and RX_p have L_p and M_p antennas, respectively.

For this work, it will be considered the uplink direction, where each UT transmits N_s data streams to its respective receiver. The received signal at RX_p is given by

$$\mathbf{y}_p = \sum_{u=0}^N \mathbf{H}_{p,u} \mathbf{x}_u + \mathbf{n}_p, \quad (16)$$



where $\mathbf{y}_p \in \mathbb{C}^{M_p}$ denotes the received signal, $\mathbf{x}_u \in \mathbb{C}^{L_u}$ the UT_u transmitted signal, $\mathbf{n}_p \in \mathbb{C}^{M_p}$ the white Gaussian noise with variance σ^2 and $\mathbf{H}_{p,u} \in \mathbb{C}^{M_p \times L_u}$ the channel between UT_u and RX_p .

5.1.1. User Terminal Architecture

For UT_u a hybrid analog-digital architecture, as depicted in Figure 5.2, is considered. In this architecture, UT_u is equipped with T_u transmitting RF chains. As such, the transmitted signal is given by

$$\mathbf{x}_u = \mathbf{W}_{a,u} \mathbf{W}_{d,u} \mathbf{s}_u, \quad (17)$$

where $\mathbf{W}_{a,u} \in \mathbb{C}^{L_u \times T_u}$ is the analog precoder, which is comprised of a number of phase-shifters that connect each RF chain to all transmit antennas, $\mathbf{W}_{d,u} \in \mathbb{C}^{T_u \times N_s}$ the digital precoder and $\mathbf{s}_u \in \mathbb{C}^{N_s}$ denotes the UT_u data symbols modulated using an M -QAM constellation. The precoders must be designed such that the power constraint $\|\mathbf{W}_{a,u} \mathbf{W}_{d,u}\|_F^2 = N_s$ is respected.

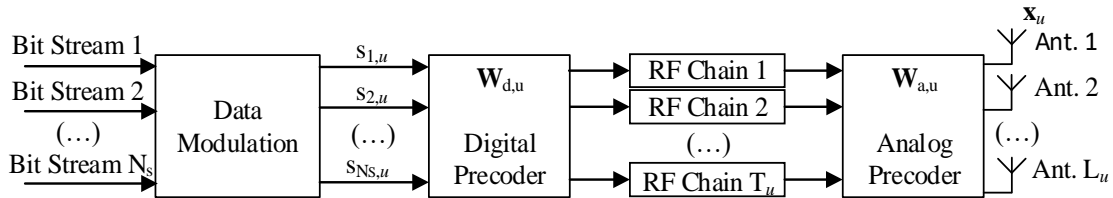


Figure 5.2. User terminal block diagram

5.1.2. Receiver Architecture

As previously mentioned, at the receiver side, the analog processing is performed at RX_p and the digital processing at the BS or CU. In the following sections, the analog and digital processing will be described in two different sections.

5.1.2.1. Analog domain

As previously mentioned at RX_p , an analog only architecture is considered (see Figure 5.3 and Figure 5.4). The RX_p has M_p antennas and outputs R_p signals to the digital



processing entity. RX_p performs a linear map between its inputs and outputs. This mapping may be mathematically described by

$$\hat{\mathbf{s}}_{a,p} = \mathbf{G}_{a,p}^H \mathbf{y}_p, \quad (18)$$

where $\hat{\mathbf{s}}_{a,p} \in \mathbb{C}^{R_p}$ denotes the vector containing the R_p outputs of RX_p and $\mathbf{G}_{a,p} \in \mathbb{C}^{M_p \times R_p}$ the analog equalizer, which is comprised of a number of phase-shifters that connect each output to all receiving antennas.

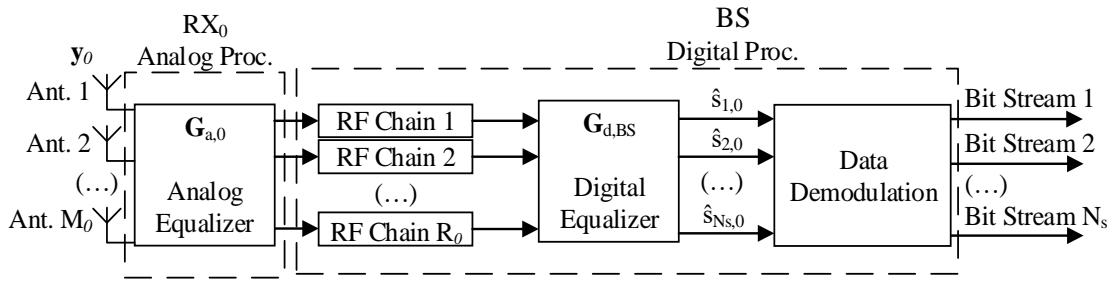


Figure 5.3. Block diagram of macro-cell receiver.

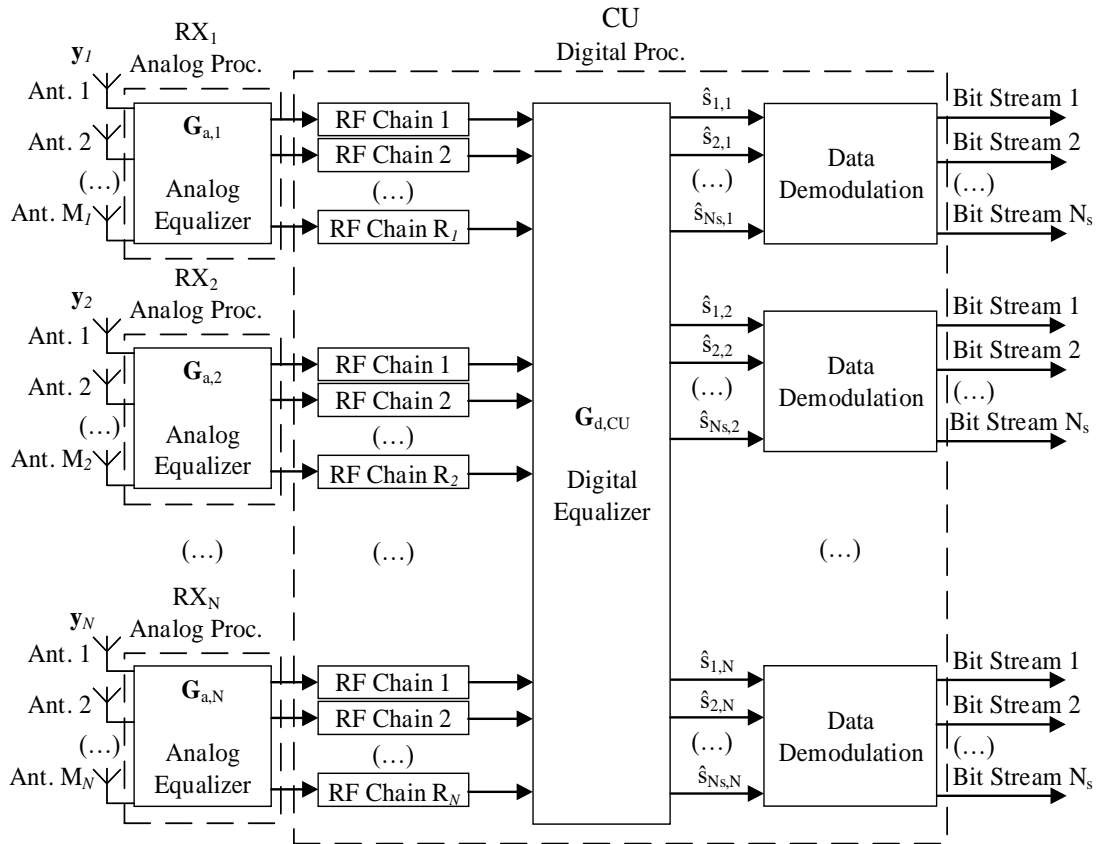


Figure 5.4. Central unit block diagram.



5.1.2.2. Digital domain

For the digital domain processing, solely the model for the CU is described, since for the BS, the description is identical to the case where the CU processes only one small cell ($N = 1$). The CU receives the signal $\hat{\mathbf{s}}_{a,CU} = [\hat{\mathbf{s}}_{a,1}^T, \dots, \hat{\mathbf{s}}_{a,N}^T]^T \in \mathbb{C}^{R_1 + \dots + R_N}$ through the front-haul. This signal is first digitized by $R_{CU} = R_1 + \dots + R_N$ RF chains and then processed by the digital equalizer at baseband frequency. The estimated symbols at the CU are given by

$$\hat{\mathbf{s}}_{d,CU} = \mathbf{G}_{d,CU}^H \hat{\mathbf{s}}_{a,CU}, \quad (19)$$

where $\hat{\mathbf{s}}_{d,CU} = [\hat{\mathbf{s}}_0^T, \dots, \hat{\mathbf{s}}_u^T, \dots, \hat{\mathbf{s}}_N^T]^T$ denotes the estimated transmitted symbols from each UT, with $\hat{\mathbf{s}}_u \in \mathbb{C}^{N_s}$ and $\mathbf{G}_{d,CU} \in \mathbb{C}^{R_{CU} \times (N+1)N_s}$ is the digital equalizer. One of the dimensions of the digital part of the equalizer is equal to the total number of streams sent by the $N+1$ UTs. Therefore, one requirement for resolvability of all streams is $R_{CU} \geq (N+1)N_s$.

5.1.3. Channel Model

For the channel model, a narrowband clustered channel based on the Saleh-Valenzuela is adopted. As discussed in [29], the channel $\mathbf{H}_{p,u}$, $p, u \in \{0, \dots, N\}$ is considered the sum of the contributions of N_{cl} scattering clusters, where each of the clusters contributes N_{ray} propagation paths to the channel matrix $\mathbf{H}_{p,u}$. The matrix channel $\mathbf{H}_{p,u}$ can be described by

$$\mathbf{H}_{p,u} = \gamma \sum_{i,l} \alpha_{il}^{p,u} \mathbf{a}_{p,u}(\phi_{il}^{p,u}, \theta_{il}^{p,u}) \mathbf{b}_{p,u}(\varphi_{il}^{p,u}, \varrho_{il}^{p,u})^*, \quad (20)$$

where $\gamma = \sqrt{N_t N_r / N_{cl} N_{ray}}$ denotes the normalization factor; $\alpha_{il}^{p,u}$ the complex gain of the i -th scattering cluster and the l th ray for the channel between UT _{u} and RX _{p} , where both $\phi_{il}^{p,u}(\theta_{il}^{p,u})$ and $\varphi_{il}^{p,u}(\varrho_{il}^{p,u})$ represent its azimuth (elevation) angles of arrival and departure for the link between RX _{p} and UT _{u} respectively; $\mathbf{a}_{p,u}$ ($\mathbf{b}_{p,u}$) the normalized receive (transmit) array response for the link between RX _{p} and UT _{u} . In the following, we will also use the matrix form of (20)



$$\mathbf{H}_{p,u} = \mathbf{A}_{p,u} \mathbf{\Lambda}_{p,u} \mathbf{B}_{p,u}^H, \quad (21)$$

where $\mathbf{\Lambda}_{p,u}$ is a diagonal matrix where the entries are given by $\{\gamma \alpha_{il}^{p,u}\}_{1 \leq i \leq N_{cl}, 1 \leq l \leq N_{ray}}$,

$$\mathbf{A}_{p,u} = [\mathbf{a}_{p,u}(\phi_{il}^{p,u}, \theta_{il}^{p,u})]_{1 \leq i \leq N_{cl}, 1 \leq l \leq N_{ray}} \quad \text{and} \quad \mathbf{B}_{p,u} = [\mathbf{b}_{p,u}(\phi_{il}^{p,u}, \vartheta_{il}^{p,u})]_{1 \leq i \leq N_{cl}, 1 \leq l \leq N_{ray}}.$$

5.2. Hybrid Precoder and Equalizer Design

In massive MIMO mmWave systems, the implementation of full digital algorithms can be impractical, as each antenna requires a dedicated RF chain. Hybrid designs are taken into consideration at both the transmitter and receiver terminals in this work. For the sake of simplicity and without loss of generality, in this section only the design of the small cell precoder and equalizer is described, since the macro-cell precoder and equalizer may be obtained using a similar approach. For the macro BS, the N small cell UTs may be considered as just one UT, since interference alignment to align the signals of these N terminals at the BS is used.

A decoupled design is considered. First, the analog part was designed, and then with the knowledge of the analog part, the digital part was also designed. Apart from simplifying the design of the analog and digital parts, this decoupled procedure brings further benefits. Namely, the channel between UT_u and RX_0 has dimensionality $L_u M_0$. By including the analog precoder and equalizer at both ends of the channel, the resulting equivalent channel has dimensionality $T_u R_0$. As the number of RF chains is much smaller than the number of antennas, then the dimensionality of the equivalent channel is much smaller than the dimensionality of the original channel. This fact significantly reduces the overhead necessary to estimate such channels, a factor that will be important in the design of the digital precoder of the small cell UTs which requires the knowledge of the inter-tier channels and uses the interference alignment technique to align the inter-tier interference along a low dimensional subspace.

5.2.1. Analog Equalizer and Precoder Design

For the analog part, two types of equalizers/precoders are proposed, one that is randomly generated and another that considers the channel information and the specific



characteristics of mmWave-channels (specifically the sparsity) to compute the analog precoder.

In the following, solely the analog equalizer design is described, since the analog precoder is similar. The main difference between the two is the value of the weighting matrix \mathbf{R} in the optimization problem (26). For the precoder, this matrix is equal to the identity but for the equalizer, it corresponds to the received signal correlation matrix.

5.2.1.1. Random Equalizer

In random design, the analog decoder is randomly generated. By doing this, the receiver does not need information about the channel, simplifying the overall system design and reducing the overhead required to estimate the channel. As the analog part is composed of a matrix of analog phase shifters, each element of the decoder must be normalized, so that $(|\mathbf{G}_{a,p}(i,j)|^2 = M_p^{-1})$. The analog equalizer may then be expressed as

$$\mathbf{G}_{a,p} = e^{i2\pi\Theta_p}, \quad (22)$$

where $\Theta_p \in \mathbb{C}^{M_p \times R_p}$ denotes a matrix of uniform random numbers, such that $\Theta_p(i,j) \in [0,1]$, with $i \in \{1, \dots, M_p\}$ and $j \in \{1, \dots, R_p\}$ and the exponential is applied element-wise to the matrix Θ_p .

5.2.1.2. Proposed Distributed Hybrid Equalizer for Heterogeneous Networks

From (18) and (19), it follows that the equalized signal at the CU is given by

$$\hat{\mathbf{s}}_{d,CU} = \mathbf{G}_{d,CU}^H \mathbf{G}_{a,CU}^H \mathbf{y}_{CU}, \quad (23)$$

where $\mathbf{G}_{a,CU} = \text{diag}(\mathbf{G}_{a,1}, \dots, \mathbf{G}_{a,N})$ and $\mathbf{y}_{CU} = [\mathbf{y}_1^T, \dots, \mathbf{y}_N^T]^T$. By (16), (17) follows that

$$\hat{\mathbf{s}}_{d,CU} = \mathbf{G}_{d,CU}^H \mathbf{G}_{a,CU}^H \mathbf{H}_{CU} \mathbf{W} \mathbf{s} + \mathbf{G}_{d,CU}^H \mathbf{G}_{a,CU}^H \mathbf{n}_{CU} \quad (24)$$

where $\mathbf{H}_{CU} = [\mathbf{H}_{p,u}]_{1 \leq p \leq N, 0 \leq u \leq N}$, $\mathbf{W} = \text{diag}(\mathbf{W}_{a,u} \mathbf{W}_{d,u})_{0 \leq u \leq N}$, $\mathbf{s} = [\mathbf{s}_u]_{0 \leq u \leq N}$ and $\mathbf{n}_{CU} = [\mathbf{n}_p]_{0 \leq p \leq N}$.

Let $\mathbf{G}_{CU,opt}$ denote the optimum fully digital equalizer. If we use as a metric the mean square error, then the optimum fully digital equalizer is the Minimum Mean Square Error (MMSE) which is given by



$$\mathbf{G}_{CU,opt} = \left(\mathbf{W}^H \mathbf{H}_{CU}^H \mathbf{H}_{CU} \mathbf{W} + \sigma^2 \mathbf{I}_{N_s} \right)^{-1} \mathbf{W}^H \mathbf{H}_{CU}^H \quad (25)$$

To optimize the analog part of the equalizer, it will be used as a metric the weighted Frobenius norm [24] between the fully digital and hybrid equalizers. Mathematically, this corresponds to

$$\begin{aligned} \mathbf{G}_{a,CU} &= \arg \min \left\| \mathbf{R}^{1/2} \left(\mathbf{G}_{CU,opt} - \mathbf{G}_{a,CU} \mathbf{G}_{d,CU}^{opt} \right) \right\|_F^2 \\ \text{s.t. } \mathbf{G}_{a,CU} &\in \mathcal{G}_a. \end{aligned} \quad (26)$$

where $\mathbf{R} = \mathbf{H}_{CU} \mathbf{W} \mathbf{W}^H \mathbf{H}_{CU}^H + \sigma^2 \mathbf{I}$ denotes the correlation matrix [24] of the signal $\mathbf{y}_{CU} = [\mathbf{y}_p]_{1 \leq p \leq N}$, and \mathcal{G}_a denotes the set of all block-diagonal matrices with block-diagonal entries respecting the analog constraint ($|\mathbf{G}_{a,p}(i, j)|^2 = M_p^{-1}$). More specifically, the set \mathcal{G}_a is given by $\mathcal{G}_a = \{ \mathbf{G}_{a,CU} : \mathbf{G}_{a,CU} = \text{diag}(\mathbf{G}_{a,p})_{1 \leq p \leq N}, |\mathbf{G}_{a,p}(i, j)|^2 = M_p^{-1}, \forall p \in \{1, \dots, N\} \}$. In this optimization problem, we considered the optimum digital part to obtain the analog part of the equalizer, which accordingly to the KKT conditions is given by

$$\mathbf{G}_{d,CU}^{opt} = \left(\mathbf{G}_{a,CU}^H \mathbf{R} \mathbf{G}_{a,CU} \right)^{-1} \mathbf{G}_{a,CU}^H \mathbf{R} \mathbf{G}_{CU,opt}. \quad (27)$$

Using (27), the optimization problem simplifies to

$$\begin{aligned} \mathbf{G}_{a,CU} &= \arg \min \left\| \mathbf{Q} \mathbf{R}^{1/2} \mathbf{G}_{CU,opt} \right\|_F^2 \\ \text{s.t. } \mathbf{G}_{a,CU} &\in \mathcal{G}_a. \end{aligned} \quad (28)$$

where $\mathbf{Q} = \mathbf{I} - \mathbf{R}^{1/2} \mathbf{G}_{a,CU} \left(\mathbf{G}_{a,CU}^H \mathbf{R} \mathbf{G}_{a,CU} \right)^{-1} \mathbf{G}_{a,CU}^H \mathbf{R}^{1/2}$. By expanding the merit function of the optimization problem (28), we verify that it is equal to a constant minus a term that is dependent on $\mathbf{G}_{a,CU}$. Therefore, (28) simplifies to

$$\begin{aligned} \mathbf{G}_{a,CU} &= \arg \max \left\| \left(\mathbf{G}_{a,CU}^H \mathbf{R} \mathbf{G}_{a,CU} \right)^{-1/2} \mathbf{G}_{a,CU}^H \mathbf{R} \mathbf{G}_{CU,opt} \right\|_F^2 \\ \text{s.t. } \mathbf{G}_{a,CU} &\in \mathcal{G}_a. \end{aligned} \quad (29)$$

To solve (29), it's proposed to iteratively optimize the analog equalizer matrix column by column. Let $\mathbf{G}_{a,CU}^{(i-1)}$ denote the output of the optimization problem at iteration $i-1$ and



$\mathbf{G}_{a,CU}^{(i)} = [\mathbf{G}_{a,CU}^{(i-1)}, \mathbf{g}_{a,CU}^{(i)}]$ where $\mathbf{g}_{a,CU}^{(i)}$ denotes the column we are optimizing at the iteration i , then, using the Gram-Schmidt orthogonalization, follows that $\mathbf{R}^{1/2} \mathbf{G}_{a,CU}^{(i)} ((\mathbf{G}_{a,CU}^{(i)})^H \mathbf{R} \mathbf{G}_{a,CU}^{(i)})^{-1/2} = [\mathbf{U}^{(i-1)}, \mathbf{P}^{(i-1)} \mathbf{R}^{1/2} \mathbf{g}_{a,CU}^{(i)}]$ with $\mathbf{P}^{(i-1)} = \mathbf{I} - \mathbf{U}^{(i-1)} \mathbf{U}^{(i-1)H}$ and $\mathbf{U}^{(i-1)} = \mathbf{R}^{1/2} \mathbf{G}_{a,CU}^{(i-1)} ((\mathbf{G}_{a,CU}^{(i-1)})^H \mathbf{R} \mathbf{G}_{a,CU}^{(i-1)})^{-1/2}$. Therefore, the objective at iteration i is to find column i of the analog equalizer, which is given by

$$\begin{aligned} & \mathbf{g}_{a,CU}^{(i)} \\ &= \arg \max \mathbf{G}_{CU,opt}^H \mathbf{R}^{H/2} (\mathbf{U}^{(i-1)} \mathbf{U}^{(i-1)H} \\ & \quad + \mathbf{P}^{(i-1)} \mathbf{R}^{1/2} \mathbf{g}_{a,CU}^{(i)} (\mathbf{g}_{a,CU}^{(i)})^H \mathbf{R}^{H/2} \mathbf{P}^{(i-1)}) \mathbf{R}^{1/2} \mathbf{G}_{CU,opt} \\ & \text{s.t. } \mathbf{g}_{a,CU}^{(i)} \in \mathcal{G}_a. \end{aligned} \quad (30)$$

and equivalent to

$$\begin{aligned} & \mathbf{g}_{a,CU}^{(i)} = \arg \max \left\| \mathbf{C}^{(i-1)} \mathbf{g}_{a,CU}^{(i)} \right\|^2, \\ & \text{s.t. } \mathbf{g}_{a,CU}^{(i)} \in \mathcal{G}_a. \end{aligned} \quad (31)$$

where $\mathbf{R}^{(i-1)} = \mathbf{R}^{H/2} \mathbf{P}^{(i-1)} \mathbf{R}^{1/2}$ and $\mathbf{C}^{(i-1)} = \mathbf{G}_{CU,opt}^H \mathbf{R}^{(i-1)}$. Accordingly, to the definition of the constraint set \mathcal{G}_a , the optimum analog equalizer must have a block diagonal structure. Let us decompose matrix $\mathbf{C}^{(i-1)}$ in N blocks along its columns, i.e., $\mathbf{C}^{(i-1)} = [\mathbf{C}_1^{(i-1)}, \dots, \mathbf{C}_p^{(i-1)}, \dots, \mathbf{C}_N^{(i-1)}]$. Then, by including the block diagonal constraint in the merit function of the optimization problem (31) follows

$$\begin{aligned} & (\mathbf{g}_{a,p}^{(i)}, p) = \arg \max \left(\max_p \left\{ \left\| \mathbf{C}_p^{(i-1)} \mathbf{g}_{a,p}^{(i)} \right\|^2 \right\} \right) \\ & \text{s.t. } \mathbf{g}_{a,p}^{(i)} \in \bar{\mathcal{G}}_a, \forall p \in 1, \dots, N \end{aligned} \quad (32)$$

where $\mathbf{g}_{a,p}^{(i)}$ denotes a column of the analog part of the equalizer of RX_p , and $\bar{\mathcal{G}}_a = \{\mathbf{g}_{a,p}^{(i)} : |\mathbf{g}_{a,p}^{(i)}|^2 = M_p^{-1}\}$. To solve (32), the optimum value of $\mathbf{g}_{a,p}^{(i)}$ is found for all $p \in \{1, \dots, N\}$ and then select the index p that corresponds to the maximum among all $p \in \{1, \dots, N\}$. For RX_p this corresponds to

$$\mathbf{g}_{a,p}^{(i)} = \arg \max \left\| \mathbf{C}_p^{(i-1)} \mathbf{g}_{a,p}^{(i)} \right\|^2, \text{ s.t. } \mathbf{g}_{a,p}^{(i)} \in \bar{\mathcal{G}}_a \quad (33)$$

Replacing the constraint $|\mathbf{g}_{a,p}^{(i)}|^2 = M_p^{-1}$ with the relaxed constraint $\|\mathbf{g}_{a,p}^{(i)}\|^2 = 1$, then the optimum value of the previous problem is equal to the maximum eigenvalue of the positive-



semidefinite matrix $(\mathbf{C}_p^{(i-1)})^H \mathbf{C}_p^{(i-1)}$, and $\mathbf{g}_{a,p}^{(i)}$ would be equal to the corresponding eigenvector. Therefore, a simple approach to ensure that the constraint $\mathbf{g}_{a,p}^{(i)} \in \bar{\mathcal{G}}_a$ is respected is to project the corresponding eigenvector along the set of vectors in the set $\mathbf{g}_{a,p}^{(i)} \in \bar{\mathcal{G}}_a$, which amounts to retaining the phase of each element of the optimum eigenvector and setting its magnitude to M_p^{-1} . A different approach to solve (33) would be to use a dictionary whose elements respect the constraint $\mathbf{g}_{a,p}^{(i)} \in \bar{\mathcal{G}}_a$ and select the best element from the dictionary as the optimum analog equalizer. Denoting by \mathcal{D}_p the dictionary used for RX_p . Therefore, the optimization problem corresponds to

$$\mathbf{g}_{a,p}^{(i)} = \arg \max_j \left\| \mathbf{C}_p^{(i-1)} \mathbf{g}_{a,p}^j \right\|^2 \quad (34)$$

where $\mathbf{g}_{a,p}^j$ denotes the element j of the dictionary \mathcal{D}_p . For the dictionary, it may use the array response matrix of RX_p , i.e., matrix $\mathbf{A}_p = [\mathbf{A}_{p,u}]_{0 \leq u \leq N}$. From the definition of matrix $\mathbf{C}_p^{(i-1)}$, its row space is identical to the column space of the channel matrix \mathbf{H}_{CU} . Therefore, a similar conclusion applies for matrices $\mathbf{C}_p^{(i-1)}$ and $\mathbf{H}_p = [\mathbf{H}_{p,u}]_{0 \leq u \leq N}$ (see definition of the channel matrix $(\mathbf{H}_{CU} = [\mathbf{H}_{p,u}]_{1 \leq p \leq N, 0 \leq u \leq N})$). Hence, from (21), it follows that matrix \mathbf{A}_p forms a good basis for the channel [24].

With the dictionary-based approach, the CU computes the analog equalizer for the N APs and then forwards to the APs the index of the R_p selected dictionary entries, or equivalently, forwards to RX_p the selected angles of arrival. In contrast, for the projection-based approach, the CU must forward to each $\text{RX}_p, p \in \{1, \dots, N\}$ the full analog equalizer matrix $G_{a,p} \in \mathbb{C}^{R_p \times M_p}$ that corresponds to $R_p \times M_p$ real numbers. Due to its lower overhead, the dictionary-based approach is superior and is the one we will use to obtain the numerical results in Section V.



The pseudo-code for the proposed algorithm is given in Algorithm 1.

Algorithm 1: The proposed hybrid multi-user linear equalizer algorithm for HetNets

Inputs: $\mathbf{G}_{CU,opt}, \mathbf{R}^{1/2}$

1. $\mathbf{P}^{(0)} = \mathbf{I}$
 2. for $i = 1: R_{CU}$
 3. $\mathbf{R}^{(i-1)} = \mathbf{R}^{H/2} \mathbf{P}^{(i-1)} \mathbf{R}^{1/2}$
 4. $\mathbf{C}^{(i-1)} = \mathbf{G}_{CU,opt}^H \mathbf{R}^{(i-1)}$
 5. for $q = 1: N$
 6. $\mathbf{\Psi}_q = \mathbf{C}_q^{(i-1)} \mathbf{A}_q$
 7. $k_q = \arg \max_{\ell=1, \dots, N_{cl} N_{ray}} (\mathbf{\Psi}_q^H \mathbf{\Psi}_q)_{\ell, \ell}$
 8. end for
 9. $p = \arg \max_{q=1, \dots, N} (\mathbf{\Psi}_q^H \mathbf{\Psi}_q)_{k_q, k_q}$
 10. $\mathbf{G}_{a,p} = [\mathbf{G}_{a,p}, \mathbf{A}_p^{(k_p)}]$
 11. $\mathbf{G}_{a,CU} = [\mathbf{G}_{a,CU}, \mathbf{A}_p^{(k_p)}]$
 12. $\mathbf{U}^{(i-1)} = \mathbf{R}^{1/2} \mathbf{G}_{a,CU}^{(i-1)} ((\mathbf{G}_{a,CU}^{(i-1)})^H \mathbf{R} \mathbf{G}_{a,CU}^{(i-1)})^{-1/2}$
 13. $\mathbf{P}^{(i-1)} = \mathbf{I} - \mathbf{U}^{(i-1)} \mathbf{U}^{(i-1)H}$
 14. end for
 15. return : $\mathbf{G}_{a,CU}, \mathbf{G}_{a,1}, \dots, \mathbf{G}_{a,N}$
-

5.2.2. Digital Equalizer Design

For the digital part of the equalizer, we use the optimum digital equalizer as in equation (27), which is repeated here for completeness.

$$\mathbf{G}_{d,CU}^{opt} = \left(\mathbf{G}_{a,CU}^H \mathbf{R} \mathbf{G}_{a,CU} \right)^{-1} \mathbf{G}_{a,CU}^H \mathbf{R} \mathbf{G}_{CU,opt}. \quad (27)$$

As previously mentioned, the analog precoder and equalizer may be designed using similar procedures, since one may be considered as a specific case of the other. In contrast, the digital parts of the hybrid precoder and equalizer perform different functions. The digital part of the equalizer separates the received data signal into data streams, and the digital part of the precoder aligns the inter-tier interference along a small dimension subspace. In the next section, the digital precoder is described.



5.2.3. Digital Precoder Design

As discussed before for ultra-dense mmWave heterogeneous systems, the inter-tier interference from the small cell UTs to the macro-cell BS impacts the network performance. Therefore, the objective is to design the digital precoders of the small cell UTs so that the inter-tier interference is removed. To enforce the zero-interference condition, the following constraint must be respected.

$$\mathbf{G}_{d,0}^H \mathbf{F}_{0,u} \mathbf{W}_{d,u} = 0, \quad (35)$$

where $\mathbf{F}_{0,u} = \mathbf{G}_{a,0}^H \mathbf{H}_{0,u} \mathbf{W}_{a,u}$ denotes the equivalent channel between the BS and UT_u, considering both analog precoder and equalizer, which dimensionality is much smaller than the one of the original channel $\mathbf{H}_{0,u}$. Let's define matrix $\mathbf{V} = \text{null}(\mathbf{G}_{d,0})$. Then, from (35) it follows that

$$\mathbf{F}_{0,u} \mathbf{W}_{d,u} = \mathbf{V}, \quad (36)$$

The space spanned by the equivalent channel, including the digital precoder, i.e., channel $\mathbf{F}_{0,u} \mathbf{W}_{d,u}$, is identical across all small cell user terminals and equal to $\mathbf{V} \in \mathbb{C}^{K_0 \times N_s}$, which is denominated by alignment direction. Therefore, the solution to the zero-interference condition is

$$\mathbf{W}_{d,u} = \text{null}(\mathbf{G}_{d,0}^H \mathbf{F}_{0,u}), \quad (37)$$

$$\mathbf{V} = \text{null}(\mathbf{G}_{d,0}), \quad (38)$$

According to the previous derivation, the alignment direction \mathbf{V} completely defines the subspace where the full inter-tier interference resides. This subspace occupies a subspace with dimensionality N_s . In contrast, if condition (35) is not respected, the interference subspace dimensionality would be NN_s , i.e., N times higher. Furthermore, from (38), we verify that the alignment direction is a function of the BS digital equalizer and vice-versa. As the UT_u, $u \in \{1, \dots, N\}$ precoder is a function of the digital equalizer of the BS (or equivalently, of the alignment direction), this matrix must be known at all UTs. Several approaches may be considered to select the value of this matrix. In the following subsections, we describe three approaches in more detail. It is assumed that this matrix is selected at the macro BS, since its value will influence the performance of the macro-cell, and then it is forwarded to the small cells through the air. By starting with the optimum approach, with the highest requirements in terms of information exchange between the macro and small



cells and then proceed until the simplest and with the lowest requirements in terms of information exchange. The approach proposed in the previous paragraphs has similarities with the one proposed in [68]. However, here we consider that the small cell UTs transmit more than one stream, and the type of architecture considered is quite different. As mentioned, we consider a hybrid analog-digital architecture in this work and in [68], a fully digital architecture was assumed.

5.2.3.1. Fully Coordinated

In the fully coordinated approach, the alignment direction \mathbf{V} is generated at the BS, and the macro-cell performance is the best. To achieve the best performance, the alignment direction, where the inter-tier interference resides, must span a subspace orthogonal to the signal space of the macro-cell signal. Mathematically, this corresponds to setting the alignment direction as follows

$$\mathbf{V} = \text{null}(\mathbf{G}_{a,0}^H \mathbf{H}_{0,0} \mathbf{W}_{a,0}). \quad (39)$$

Equation (39) ensures that no attenuation occurs in the desired signal when the interference is removed. To compute \mathbf{V} , the analog precoder and equalizer of the macro-cell terminals must be previously computed or have access to some knowledge about them. However, as the alignment direction must be fed back to the secondary system at each transmission time interval (TTI), the feedback requirements can be quite demanding, at $2R_0 N_s$ reals per TTI.

5.2.3.2. Static

In the static method, the alignment direction is predefined and does not change throughout the communication process. The alignment direction needs to be shared just once, at the beginning of the interaction. This implies a reduction in the performance, but the feedback requirements are greatly reduced.

5.2.3.3. 2n-Bit Coordinated

In [69], the authors propose a $2n$ -bit coordinated method where it is possible to achieve a compromise between performance and feedback requirements, ranging from the static method ($n=0$) to the fully coordinated method ($n=\infty$). In this method, the alignment direction is obtained as in the fully coordinated method. However, instead of feeding back real numbers, only a quantized version of the alignment direction matrix is fed back. This



quantized version feeds back n bits from the real part and other n bits from the complex part. Hence the $2n$ -bit name, where $n=1,2,3$. The quantized alignment direction matrix is given by

$$\mathbf{V}_q = f_q(\text{Re}\{\mathbf{V}\}) + i f_q(\text{Im}\{\mathbf{V}\}), \quad (40)$$

where $f_q(\cdot)$ denotes the quantization function, and $\text{Re}\{\cdot\}$ and $\text{Im}\{\cdot\}$ the real and complex parts of the alignment direction \mathbf{V} .

As seen in [69] for a flat fading Rayleigh channel without spatial correlation and with independent channel realizations, 1 bit for each real and complex part of the IA vector ($n = 1$) shows promising results for a minimum feedback requirement. For this specific case, the channel is correlated along the spatial dimension and not Rayleigh-distributed. It is a narrowband clustered channel as described in section II.C. However, as will be verified in the numerical results section, the performance of the 1-bit scheme is close to the full-coordinated approach.

5.3. Simulation and Results

In this section, a comparison of the performance results for different combinations of the previously described precoder and equalizer designs is made. Two scenarios are considered with the main parameters shown in TABLE 5.I, each with six different schemes, as seen in TABLE 5.II. The main difference between scenario 1 and 2 is that the number of transmitting data streams of the second is twice the first.

TABLE 5.I: Parameters for the two different scenarios.

Parameters	N_s	N	M_p	M_s	L_p	L_s	T_p	T_s	R_p	R_s
Scenario 1	1	2	32	16	16	16	1	2	2	2
Scenario 2	2	2	32	16	16	16	2	4	4	4



TABLE 5.II: Precoder/equalizer designs.

Scheme	Analog Precoder	Analog Equalizer	Small/Macro Cell	Alignment Direction
1	Random	Random		Static
2	Random	Random		2 bit
3	Random	Algorithm 1		2 bit
4	Algorithm 1	Algorithm 1		2 bit
5	Algorithm 1	Algorithm 1		Full-Coordinated
6			Full Digital	

In all schemes, (28) is used to compute the digital part of the equalizers (either BS or CU). The first precoder/equalizer scheme corresponds to the case where both analog precoders and equalizers are randomly generated as in (23), and the static method for the digital small cells UT precoders. With this scheme, the system has the minimum inter-system feedback requirements, since the alignment direction must be shared only once. In the second scheme, the static IA vector is replaced by the coordinated vector, with 2 ($n=1$) quantization bits. In the third scheme, the random analog equalizer at both the small cell BS and macro-cell APs is replaced by the proposed algorithm, described in chapter 5.2.1 (Algorithm 1). In this case, the BS and the CU must estimate a channel with higher dimension than the previous scenarios. In the fourth scheme, the random analog precoder is replaced by the proposed algorithm. In this case, the UTs need to know more information about the channel regarding the previous scenarios. In the fifth scheme, the static IA vector is replaced by the full coordinated approach, where the inter-tier exchange information is the highest. Finally, at the sixth scheme, a fully digital system is considered, i.e., one RF chain is assumed per antenna, and the IA vector is computed based on a full coordinated approach.

For the channel model, $N_{cl} = 8$ clusters are considered, all with the same average power and each with $N_{ray} = 3$ rays with Laplacian distributed azimuth/elevation angles of arrival/departure as in [70]. The angle spread for both the transmitter and receiver is 8° . Although it was used this specific value, similar results are obtained for larger angle spreads. The carrier frequency is set to 28 GHz, and the antenna spacing elements assumed to be half-



wavelength. All results were obtained by considering QPSK modulation. The performance metric considered is the BER, which is presented as a function of the E_b / N_0 , with E_b denoting the average bit energy and N_0 denoting the one-sided noise power spectral density, given by $E_b / N_0 = 1 / (2\sigma^2)$. Let's start by analyzing scenario 1. In Figure 5.5, the results for the macro-cell are presented, while Figure 5.6 shows the results for the small cell. From Figure 5.5, it can be seen that the performance is the worst for the first scheme since the analog precoders and equalizer are randomly generated, and the alignment vector is static. These results are expected since the information about the channels at the terminals is quite small. We can observe that just by using a 2-bit quantization of the alignment vector, scheme 2, the performance improves 10.6 dB for a BER= 10^{-3} . The results also show that by using the proposed analog equalizer, scheme 3, the performance improves 15.9 dB for the same BER and by further using the proposed precoder, scheme 4, the performance improves 11 dB for a BER= 10^{-3} . By replacing the 2-bit approach (low overhead) with the full coordinated (high overhead), scheme 5, the improvement is small. It can also be seen that the performance of the proposed analog equalizer/precoder with a 2-bit quantization for the alignment (scheme 5) is very close the one achieved by the full coordinated approach, that can be seen as the lower bound for the analog-digital approaches, indicating that the proposed hybrid scheme is quite efficient to remove the interference that the small cell UTs cause in the macro-cell BS using the degrees of freedom of the mmWave channel efficiently.

Figure 5.6 (small cell results) shows that the performance of the scheme 1 and 2 is the same as in scheme 4 and 5. From Table II, we can see that for these two pairs of schemes (scheme 1, 2 and scheme 4, 5), the analog equalizer and precoders are the same, only the alignment direction changes as a result of the independence between macro and small cell channels, which are used to compute the alignment direction and the precoders/equalizers, respectively. Similar to the macro case, scheme 5 has the best performance, which is identical to the scheme 4 as previously discussed. Again, the gap between the proposed hybrid scheme and the full digital approach is very small, which means that the proposed distributed scheme effectively mitigates the multiuser and inter-tier interferences

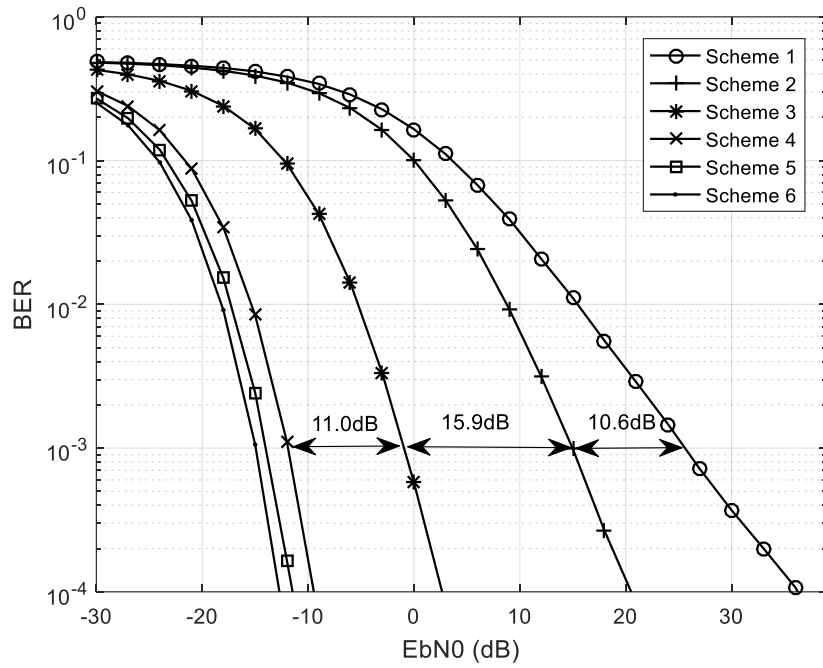


Figure 5.5. Macro-cell average BER for the first scenario.

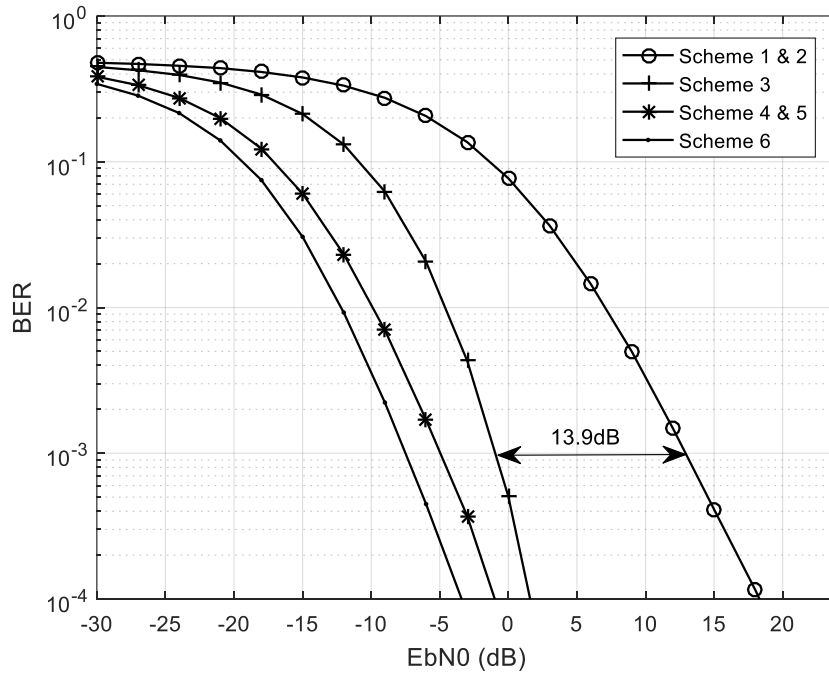


Figure 5.6. Small cell average BER for the first scenario.



The results for scenario 2 are depicted in Figure 5.7 and Figure 5.8 for macro and small cells, respectively. In this case, the number of transmitting data streams is twice the number of the first scenario, i.e., each UT transmits 2 data symbols in parallel. From these figures, we basically can note conclusions similar to scenario 1. From Figure 5.7 (macro-cell results), it can be seen that by replacing the 2-bit quantization approach (scheme 4) with the full coordinated approach (scheme 5), the improvement is more significant than in the scenario 1, i.e., the gap between these two schemes is larger than in the first scenario. Therefore, scenario 2 requires more bits to approach the full coordinated approach and hence a higher overhead because now the level of interference is higher since the intra-tier interference is composed of the intersymbol and multi-user interference, contrary to scenario 1 which has only multi-user interference.

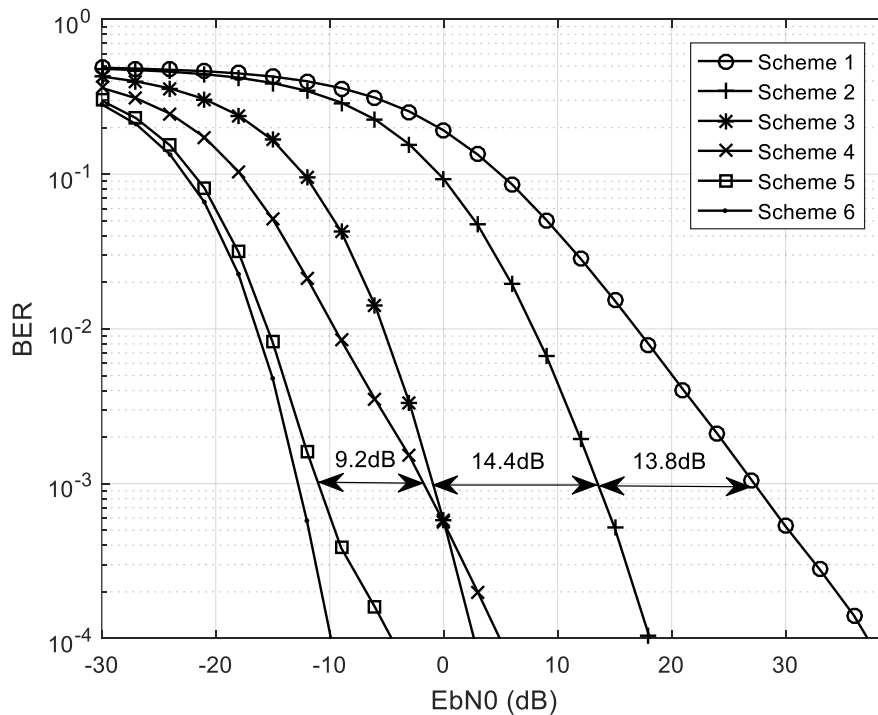


Figure 5.7. Macro-cell average BER for the second scenario.

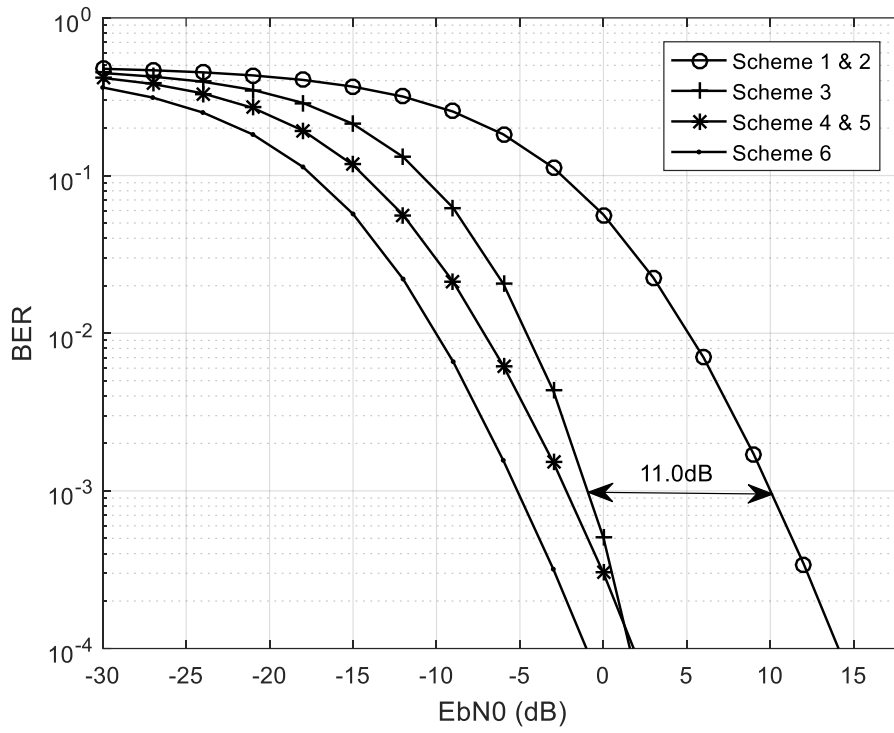


Figure 5.8. Small-cell average BER for the second scenario.



Chapter 6

Conclusion and Future Work

The introduction of LTE-Advanced in the mobile communications market, improved our experience with mobile phones. It allowed the use of countless broadband services that are already part of our daily routine. This is possible due to the technologies used in LTE-Advanced, such as MIMO and HetNets, which allows to achieve increased capacity and better coverage. However, to keep up with these increasing demands, towards 5G, new technologies are needed. Here, massive MIMO and mmWave communications may play an important role, due to their potential. Nevertheless, research is needed, as the application of these technologies for mobile communications is rather new. Future systems may be comprised of HetNets with massive MIMO and mmWave. Research in this field is needed, as the interference in HetNets is a current problem and massive MIMO with mmWave environments still require further research.

6.1. Conclusion

In this dissertation, it was proposed low-feedback overhead hybrid analog-digital precoder and equalizer schemes for the uplink in massive MIMO mmWave HetNets systems, which contributed to the advancement of the state of the art. The hybrid processing is performed in a distributed fashion at the small cells, where the analog part is performed at the small cell base stations (or Aps) and the digital part at the CU for joint processing to efficiently remove the inter/intra tier interferences. In order to optimize the analog part of the hybrid equalizer and the precoders (used at the user terminals), the



distance between the hybrid and the fully digital approaches was minimized. In the optimization problem, it was imposed constraints of the analog part and the constraints inherent to distributed nature of the APs. To cancel the inter-tier interference, the digital part of the precoders employed at the small cell user terminals was designed in such a way that this interference resides in a low dimension subspace at the macro BS.

From this work, the following conclusion can be made:

- The performance of the proposed hybrid analog-digital precoder/equalizer schemes by exploring the degrees of freedom of the mmWave channel, efficiently removes the interference caused by the small-cell UTs in the macro-BS, achieving results quite close to its fully digital counterpart when transmitting a single data symbol, as in scenario 1 of the developed work.
- In a scenario where a single or a small number of parallel data symbols are transmitted, as in scenarios 1 and 2 of the developed work, 2 bits of inter-tier information exchange are enough to efficiently align the interferences. Since the performance of the proposed schemes does not deviate much from the fully digital one. This greatly reduces the necessary overhead, consequently easing the demands on the network, achieving a good overall network performance.
- For a greater number of transmitting parallel data symbols, the system's complexity increases, and so does the level of interference. This interference is composed of intersymbol and multi-user interference. As such, for the same number of bits, the gap in the performance between the proposed scheme and the fully digital one increases with the number of data streams. Therefore, more inter-tier information bits are necessary to shorten this gap, increasing the necessary overhead and putting more strain into the system's network.

6.2. Future Work

In this work, a scenario with a single-user per cell with perfect CSI knowledge at the transmitter was considered. As future work, a more realistic scenario should be taken into account, where no perfect CSI is known at the transmitter, as well as multiple users per cell, to fully exploit multi-user MIMO techniques. Additionally, as single carrier was considered, the system could be extended to OFDM.

References

- [1] Qualcomm, “The Evolution of Mobile Technologies: 1G - 4G LTE,” no. June, pp. 1–41, 2014.
- [2] “AT&T 2G Network Shutdown - Wireless Support.” [Online]. Available: <https://www.att.com/esupport/article.html#!/wireless/KM1084805>. [Accessed: 10-Nov-2017].
- [3] “Telstra says goodbye to 2G - Telco/ISP - iTnews.” [Online]. Available: <https://www.itnews.com.au/news/telstra-says-goodbye-to-2g-443018>. [Accessed: 10-Nov-2017].
- [4] Source: 5G Americas | Statista 2017, “Global mobile subscriptions by technology 2010-2017.” [Online]. Available: <https://www.statista.com/statistics/206604/global-wireless-subscription-growth-by-technology-since-2010/>. [Accessed: 10-Nov-2017].
- [5] ITU, “IMT Vision – Framework and overall objectives of the future development of IMT for 2020 and beyond, M Series, Recommendation ITU-R M.2083-0,” vol. 0, p. 21, 2015.
- [6] Q. Technologies, “Making 5G NR a reality Transforming our world,” no. December, 2016.
- [7] N. Bhushan *et al.*, “Network densification: The dominant theme for wireless evolution into 5G,” *IEEE Commun. Mag.*, vol. 52, no. 2, pp. 82–89, 2014.
- [8] B. Romanous, N. Bitar, A. Imran, and H. Refai, “Network densification: Challenges and opportunities in enabling 5G,” *2015 IEEE 20th Int. Work. Comput. Aided Model. Des. Commun. Links Networks, CAMAD 2015*, no. I, pp. 129–134, 2016.
- [9] Z. Zhang, X. Chai, K. Long, A. V. Vasilakos, and L. Hanzo, “Full duplex techniques for 5G networks: Self-interference cancellation, protocol design, and relay selection,” *IEEE Commun. Mag.*, vol. 53, no. 5, pp. 128–137, 2015.
- [10] X. Shen, “Device-to-device communication in 5G cellular networks,” *IEEE Netw.*,

References

- vol. 29, no. 2, pp. 2–3, 2015.
- [11] T. S. Rappaport *et al.*, “Millimeter wave mobile communications for 5G cellular: It will work!,” *IEEE Access*, vol. 1, pp. 335–349, 2013.
- [12] E. Larsson, O. Edfors, F. Tufvesson, and T. Marzetta, “Massive MIMO for next generation wireless systems,” *IEEE Commun. Mag.*, vol. 52, no. 2, pp. 186–195, 2014.
- [13] K. Joshi and T. Benson, “Network Function Virtualization,” *IEEE Internet Comput.*, vol. 20, no. 6, pp. 7–9, 2016.
- [14] X. Hong, J. Wang, C. X. Wang, and J. Shi, “Cognitive radio in 5G: A perspective on energy-spectral efficiency trade-off,” *IEEE Commun. Mag.*, vol. 52, no. 7, pp. 46–53, 2014.
- [15] M. Nohrborg, “LTE.” [Online]. Available: <http://www.3gpp.org/technologies/keywords-acronyms/98-lte>. [Accessed: 28-Oct-2017].
- [16] F. Boccardi, R. Heath, A. Lozano, T. Marzetta, and P. Popovski, “Five disruptive technology directions for 5G,” *IEEE Commun. Mag.*, vol. 52, no. 2, pp. 74–80, Feb. 2014.
- [17] S. Rangan, T. S. Rappaport, and E. Erkip, “Millimeter-wave cellular wireless networks: Potentials and challenges,” *Proc. IEEE*, vol. 102, no. 3, pp. 366–385, 2014.
- [18] T. E. Bogale and L. B. Le, “Massive MIMO and mmWave for 5G Wireless HetNet: Potential Benefits and Challenges,” *IEEE Veh. Technol. Mag.*, vol. 11, no. 1, pp. 64–75, Mar. 2016.
- [19] T. S. Rappaport, F. Gutierrez, E. Ben-Dor, J. N. Murdock, Y. Qiao, and J. I. Tamir, “Broadband Millimeter-Wave Propagation Measurements and Models Using Adaptive-Beam Antennas for Outdoor Urban Cellular Communications,” *IEEE Trans. Antennas Propag.*, vol. 61, no. 4, pp. 1850–1859, Apr. 2013.
- [20] T. S. Rappaport, G. R. MacCartney, M. K. Samimi, and S. Sun, “Wideband Millimeter-Wave Propagation Measurements and Channel Models for Future Wireless Communication System Design,” *IEEE Trans. Commun.*, vol. 63, no. 9,

-
- pp. 3029–3056, Sep. 2015.
- [21] A. Alkhateeb, Jianhua Mo, N. Gonzalez-Prelcic, and R. W. Heath, “MIMO Precoding and Combining Solutions for Millimeter-Wave Systems,” *IEEE Commun. Mag.*, vol. 52, no. 12, pp. 122–131, Dec. 2014.
- [22] A. L. Swindlehurst, E. Ayanoglu, P. Heydari, and F. Capolino, “Millimeter-wave massive MIMO: the next wireless revolution?,” *IEEE Commun. Mag.*, vol. 52, no. 9, pp. 56–62, Sep. 2014.
- [23] T. S. Rappaport, *Millimeter wave wireless communications*. Prentice Hall, 2014.
- [24] O. El Ayach, S. Rajagopal, S. Abu-Surra, Z. Pi, and R. W. Heath, “Spatially Sparse Precoding in Millimeter Wave MIMO Systems,” *IEEE Trans. Wirel. Commun.*, vol. 13, no. 3, pp. 1499–1513, Mar. 2014.
- [25] J. Li, L. Xiao, X. Xu, and S. Zhou, “Robust and Low Complexity Hybrid Beamforming for Uplink Multiuser MmWave MIMO Systems,” *IEEE Commun. Lett.*, vol. 20, no. 6, pp. 1140–1143, Jun. 2016.
- [26] A. Alkhateeb and R. W. Heath, “Frequency Selective Hybrid Precoding for Limited Feedback Millimeter Wave Systems,” *IEEE Trans. Commun.*, vol. 64, no. 5, pp. 1801–1818, May 2016.
- [27] R. Magueta, D. Castanheira, A. Silva, R. Dinis, and A. Gameiro, “Hybrid Iterative Space-Time Equalization for Multi-User mmW Massive MIMO Systems,” *IEEE Trans. Commun.*, vol. 65, no. 2, pp. 608–620, Feb. 2017.
- [28] G. Xu, C.-H. Lin, W. Ma, S. Chen, and C.-Y. Chi, “Outage Constrained Robust Hybrid Coordinated Beamforming for Massive MIMO Enabled Heterogeneous Cellular Networks,” *IEEE Access*, vol. 5, pp. 13601–13616, 2017.
- [29] T. Bai and R. W. Heath, “Coverage and Rate Analysis for Millimeter-Wave Cellular Networks,” *IEEE Trans. Wirel. Commun.*, vol. 14, no. 2, pp. 1100–1114, Feb. 2015.
- [30] D. Castanheira, P. Lopes, A. Silva, and A. Gameiro, “Hybrid Beamforming Designs for Massive MIMO Millimeter-Wave Heterogeneous Systems,” *IEEE Access*, vol. 5, pp. 21806–21817, 2017.
- [31] G. Abed, M. Ismail, and K. Jumari, “Improvement of TCP Congestion Window

References

- over LTE-Advanced Networks,” *Int. J. Adv. Res. Comput. Commun. Eng.*, vol. 1, no. 4, pp. 185–192, 2012.
- [32] R. van. Nee and R. Prasad, *OFDM for wireless multimedia communications*. Artech House, 2000.
- [33] “An Introduction To Orthogonal Frequency Division Multiplex (OFDM).” [Online]. Available: <https://www.nutaq.com/blog/introduction-orthogonal-frequency-division-multiplex-ofdm>. [Accessed: 19-Oct-2017].
- [34] A. Silva and A. Gameiro, “OFDM /OFDMA, SC-FDMA and MC-CDMA Techniques,” 2016.
- [35] I. Poole, “LTE Frame Structure | Frame Subframe Type 1 & 2 | Tutorial - Radio-Electronics.Com.” [Online]. Available: <http://www.radio-electronics.com/info/cellulartelecomms/lte-long-term-evolution/lte-frame-subframe-structure.php>. [Accessed: 21-Oct-2017].
- [36] Keysight Technologies, “LTE Physical Layer Overview.” [Online]. Available: http://rfmw.em.keysight.com/wireless/helpfiles/89600b/webhelp/Subsystems/lte/content/lte_overview.htm. [Accessed: 21-Oct-2017].
- [37] H. G. Myung, J. Lim, and D. J. Goodman, “Single carrier FDMA for uplink wireless transmission,” *IEEE Veh. Technol. Mag.*, vol. 1, no. 3, pp. 30–38, 2006.
- [38] F. Mlinarsky, “LTE Physical Layer Fundamentals and Test Requirements,” 2009.
- [39] J. Wannstrom, “Carrier Aggregation explained,” 2013. [Online]. Available: <http://www.3gpp.org/technologies/keywords-acronyms/101-carrier-aggregation-explained>. [Accessed: 23-Oct-2017].
- [40] J. Wannstrom, “LTE-Advanced.” [Online]. Available: <http://www.3gpp.org/technologies/keywords-acronyms/97-lte-advanced>. [Accessed: 28-Oct-2017].
- [41] Artiza Networks, “LTE-A Tutorial: CoMP Techniques.” [Online]. Available: http://www.artizanetworks.com/resources/tutorials/acclera_tech.html. [Accessed: 18-Nov-2017].
- [42] H. Taoka, S. Nagata, K. Takeda, Y. Kakishima, X. She, and K. Kusume, “MIMO and CoMP in LTE-Advanced,” *NTT DOCOMO Tech. J.*, vol. 12, no. 2, pp. 20–28,

- 2010.
- [43] D. Lopez-Perez, I. Guvenc, G. de la Roche, M. Kountouris, T. Quek, and J. Zhang, “Enhanced intercell interference coordination challenges in heterogeneous networks,” *IEEE Wirel. Commun.*, vol. 18, no. 3, pp. 22–30, Jun. 2011.
- [44] Fujitsu, “High-Capacity Indoor Wireless Solutions: Picocell or Femtocell,” *Fujitsu White Pap.*, p. 10, 2013.
- [45] Andrew pmk, “(SVG version of Frequency_reuse.fig by Mozzerati) [CC BY-SA 2.5 (<https://creativecommons.org/licenses/by-sa/2.5>)], via Wikimedia Commons,” 2011. [Online]. Available: <http://www.mobileindonesia.net/frequency-reuse/>.
- [46] A. Damnjanovic *et al.*, “A survey on 3GPP heterogeneous networks,” *IEEE Wirel. Commun.*, vol. 18, no. 3, pp. 10–21, Jun. 2011.
- [47] C. E. Shannon, “A Mathematical Theory of Communication,” *Bell Syst. Tech. J.*, vol. 27, pp. 379–423, 623–659, 1948.
- [48] R. E. Ziemer and R. L. Peterson, *Introduction to digital communication*. Prentice Hall, 2001.
- [49] B. Vucetic and J. Yuan, *Space-time coding*. Wiley, 2003.
- [50] E. A. Neasmith and N. C. Beaulieu, “New Results on Selection Diversity,” *IEEE Trans. Commun.*, vol. 46, no. 5, 1998.
- [51] A. Silva, Adão, Gameiro, “Multiple Antenna Systems,” Aveiro, 2009.
- [52] D. Tse and P. Viswanath, *Fundamentals of wireless communication*. Cambridge University Press, 2005.
- [53] J. G. Proakis, *Digital communications*. McGraw-Hill, 2001.
- [54] J. W. Mark and W. Zhuang, *Wireless communications and networking*. Prentice Hall, 2003.
- [55] MITSUBISHI ELECTRIC CORPORATION PUBLIC RELATIONS DIVISION, “Mitsubishi Electric’s New Multibeam Multiplexing 5G Technology Achieves 20Gbps Throughput.”
- [56] T. L. Marzetta, “Massive MIMO: An Introduction,” *Bell Labs Tech. J.*, vol. 20, pp. 11–22, 2015.

References

- [57] T. L. Marzetta and B. M. Hochwald, "Fast transfer of channel state information in wireless systems," *IEEE Trans. Signal Process.*, vol. 54, no. 4, pp. 1268–1278, Apr. 2006.
- [58] T. S. Rappaport, *Wireless communications : principles and practice*. Dorling Kindersley, 2009.
- [59] Lili Wei, R. Hu, Yi Qian, and Geng Wu, "Key elements to enable millimeter wave communications for 5G wireless systems," *IEEE Wirel. Commun.*, vol. 21, no. 6, pp. 136–143, Dec. 2014.
- [60] J. Rosen and L. Q. Gothard, *Encyclopedia of physical science*. Facts On File, 2010.
- [61] C. A. Levis, Levis, and C. A., "Friis Free-Space Transmission Formula," in *Wiley Encyclopedia of Electrical and Electronics Engineering*, Hoboken, NJ, USA: John Wiley & Sons, Inc., 1999.
- [62] C. R. Anderson and T. S. Rappaport, "In-Building Wideband Partition Loss Measurements at 2.5 and 60 GHz," *IEEE Trans. Wirel. Commun.*, vol. 3, no. 3, pp. 922–928, May 2004.
- [63] T. S. Rappaport, J. N. Murdock, and F. Gutierrez, "State of the Art in 60-GHz Integrated Circuits and Systems for Wireless Communications," *Proc. IEEE*, vol. 99, no. 8, pp. 1390–1436, Aug. 2011.
- [64] Shu Sun and T. S. Rappaport, "Multi-beam antenna combining for 28 GHz cellular link improvement in urban environments," in *2013 IEEE Global Communications Conference (GLOBECOM)*, 2013, pp. 3754–3759.
- [65] V. Va and R. W. Heath, "Basic Relationship between Channel Coherence Time and Beamwidth in Vehicular Channels," in *2015 IEEE 82nd Vehicular Technology Conference (VTC2015-Fall)*, 2015, pp. 1–5.
- [66] T. E. Bogale and L. B. Le, "Massive MIMO and Millimeter Wave for 5G Wireless HetNet: Potentials and Challenges," Oct. 2015.
- [67] R. W. Heath, N. Gonzalez-Prelcic, S. Rangan, W. Roh, and A. M. Sayeed, "An Overview of Signal Processing Techniques for Millimeter Wave MIMO Systems," *IEEE J. Sel. Top. Signal Process.*, vol. 10, no. 3, pp. 436–453, Apr. 2016.
- [68] D. Castanheira, A. Silva, and A. Gameiro, "Set Optimization for Efficient

References

- Interference Alignment in Heterogeneous Networks,” *IEEE Trans. Wirel. Commun.*, vol. 13, no. 10, pp. 5648–5660, Oct. 2014.
- [69] S. S. Ali, D. Castanheira, A. Silva, and A. Gameiro, “Joint signal alignment precoding and physical network coding for heterogeneous networks,” *Phys. Commun.*, vol. 23, no. C, pp. 125–133, Jun. 2017.
- [70] G. Wang, J. Sun, and G. Ascheid, “Hybrid Beamforming with Time Delay Compensation for Millimeter Wave MIMO Frequency Selective Channels,” in *2016 IEEE 83rd Vehicular Technology Conference (VTC Spring)*, 2016, pp. 1–6.